Multiquantum states derived from Davydov's $|D_1\rangle$ *ansatz*: II. An exact special case solution for the Su-Schrieffer-Heeger Hamiltonian and its relation to the $|\Phi_2\rangle$ state

1998 J. Phys.: Condens. Matter 10 2631

(http://iopscience.iop.org/0953-8984/10/12/007)

J. Phys.: Condens. Matter **10** (1998) 2631–2662. Printed in the UK PII: S0953-8984(98)87204-4

Multiquantum states derived from Davydov's $|D_1\rangle$ *ansatz*: II. An exact special case solution for the Su–Schrieffer–Heeger Hamiltonian and its relation to the $|\Phi_2\rangle$ state

Wolfgang Förner

Box 2016, Chemistry Department, King Fahd University of Petroleum and Minerals, Dhahran 31261, Saudi Arabia†, and Chair for Theoretical Chemistry, Friedrich-Alexander University Erlangen–Nürnberg, Egerlandstrasse 3, D-91058 Erlangen, Germany

Received 27 August 1997, in final form 26 November 1997

Abstract. We present the derivation of an exact special case solution (for a classical lattice) for the Su–Schrieffer–Heeger model for the calculation of soliton dynamics in *trans*-polyacetylene. Our solution is exact, in the sense that the *ansatz* state yields an exact solution provided that the equations of motion for its parameters are obeyed. However, these equations can be solved only numerically (in principle to any desired accuracy), not analytically. The model is applied to time simulations of neutral solitons as a function of temperature. We find agreement of the results of our time simulations with experimental data on the mobility of neutral solitons in the system. Comparative calculations using the completely adiabatic model indicate that the results of this model are at variance both with experiment and with those of our model. A simple consideration of the potential barriers for soliton displacement leads to an overestimation of the soliton mobility for low temperatures and an underestimation for higher ones. In an appendix we discuss in some detail the relationship of this exact solution with the $|\Phi_2\rangle$ state *ansatz* as presented in our previous paper. We find that the *ansatz* state and the exact solution yield identical results for lattice momenta, displacements and site occupancies, but differ in a time dependent phase factor. Thus spectra computed with the dynamics resulting from the exact solution for the classical lattice on one hand and from the *ansatz* state on the other would differ from each other.

1. Introduction

Since the introduction of the soliton model and the Su–Schrieffer–Heeger (SSH) Hamiltonian [1] (for a recent comprehensive review see the article of Heeger, Kivelson, Schrieffer and Su [1]) for the explanation of various properties of *trans*-polyacetylene (*t*-PA), it has been shown that it is necessary to go beyond the simple Hückel type SSH model (see the introduction of our previous paper (appendix B) and [2–8, 20]). However, for the purpose of describing just the evolution of the chain geometry and the corresponding α-spin densities in time it seems to be sufficient to use the SSH model Hamiltonian. For this purpose a reduced value of the dimerization parameter (see section 2) u_0 has to be used to account for the shrinking of the neutral soliton width upon inclusion of electron–electron interactions.

The computation of the gradient of the electronic energy with respect to the geometrical degrees of freedom can be done in a time consuming way by a small shift of the coordinate

† Permanent address.

0953-8984/98/122631+32$19.50

of each CH unit [9–12]; however, the use of exact analytical gradients is more efficient [13]. In *t*-PA the soliton movement is restricted to less than 50 C–C bonds [2] probably due to impurities, crosslinks and *cis*-PA segments [14] or interchain interactions. Thus an open chain seems to be a more realistic model than a cyclic one. Details about the different approximations for the calculation of electronic wave functions in the framework of the Pariser–Parr–Pople (PPP) Hamiltonian, as well as about work on the influence of impurities and interchain interactions on soliton properties can be found in [15–20].

Since in all our studies using the PPP Hamiltonian we found a rather small soliton half width of about two to three lattice sites the question of the influence of quantum effects on soliton dynamics in the lattice arises (see also the review by Heeger *et al* [1]). In [71] we have derived equations of motion for *ansatz* states which include quantum effects in the lattice. Details of earlier studies on this problem in *trans*-PA and in the Davydov model for proteins can be found in [21–36] and a short discussion in the introduction of [71].

The application of Heller's formula for the calculation of vibrational spectra from dynamical simulations [37] is briefly discussed in section 2.4. A discussion on the possibilities of applying our methodology as a general concept in theoretical materials science to predict properties of charge carriers in conjugated polymers together with examples is given in [36] (second paper). Further we want to mention here that *ab initio* density functional methods (see for example [38] for semiempirical applications, [39] for applications to polyparaphenylene) can be used to study the stability of such polymers against oxidation in air theoretically. Examples of some of the different functionals developed can be found in [40–45].

The importance of conjugated polymers arises from the fact that they become electric conductors upon doping, with conductivities up to the range of copper (synthetic metals). Further, they are easily processible. The conductivity is usually attributed to a number of different nonlinear quasi-particles as charge carriers, for example, charged solitons, polarons or bipolarons, depending on the nature of the ground state of a given polymer. In some of the materials even the nature of these nonlinear excitations is still controversial. Our general aim is to develop a methodology (see [36], second paper), which is able to produce quantitatively correct answers to questions about form, stability and the motion of such quasi-particles, without using a large amount of computer time or memory. In this way it should be possible to reach theoretical predictions about useful candidates for synthetic metals. Important *ab initio* investigations on the search for low-gap polymers (in different directions regarding the chemical structure) were reported by Bakshi *et al* [46–51]. For a comprehensive review of the large amount of work performed by the group of Ladik on this topic see [52]. More complete lists of references on this topic, where many more groups are active, can be found in the review of Heeger, Kivelson, Schrieffer and Su (HKSS) [1] and in our paper on *t*-PA [36].

The present paper is structured as follows. In section 2.1 we describe briefly the general idea of solitons in *trans*-polyacetylene and the Su–Schrieffer–Heeger Hamiltonian for their description. In section 2.2 we derive a special case solution of this model for a classical lattice. We show in detail that our *ansatz* yields an exact solution, provided that the equations of motion for its parameters are obeyed. However, these equations can be solved only numerically, in principle to any desired accuracy. In section 2.3 we describe briefly the procedure for a completely adiabatic treatment, while in section 2.4 we outline how vibrational spectra can be calculated from the time simulations obtained with our method. We point out that with the adiabatic treatment such spectra cannot be calculated. Calculations of spectra along these lines will be the subject of a forthcoming paper. In section 3.1 we present the application of our solution to simulate the temperature dependence of the time

evolution of a neutral soliton initially at rest. Section 3.2 deals with the corresponding calculations using the completely adiabatic model. We show that with this model results are obtained which depend heavily on the size of the time step used and which are at variance with experiments and with those calculated with our solution. The results are summarized and discussed in section 4. In appendix A we derive in detail the equations of motion for the $|\Phi_2\rangle$ state *ansatz* [71] which is the multi-quantum analogue of Davydov's $|D_2\rangle$ state applied to fermions instead of bosons (which makes no difference in one-particle models like the SSH one). Our methodology is outlined here on the example of the prototype of the synthetic metals, namely the *trans*-polyacetylene (*t*-PA). However, we point out that it is not restricted to *t*-PA. A rather similar set of equations of motion is discussed extensively by Kopidakis *et al* [53], however, for a Hamiltonian which contains the electron–phonon coupling not in the first-neighbour part, but as an on-site term. This Hamiltonian is completely identical to Davydov's electrosoliton model and cannot be applied to polyacetylene, where the electron–phonon coupling is definitely contained in the resonance integrals, while the constant on-site terms are usually shifted to zero. Due to the fact that results derived from an electrosoliton model and those from an off-site electron–phonon coupling usually differ completely, the results presented by Kopidakis *et al* [53] cannot be compared to ours.

2. Method

2.1. The Su–Schrieffer–Heeger (SSH) Hamiltonian

One of the basic facts which had to be explained (see [1] for example) is the presence of an EPR (electron paramagnetic resonance) line with reduced width in undoped samples. This is attributed [1] to the presence of mobile spins (approximately one spin per 3000 C–H units) in the pristine material. Further we have a spinless charge transport in lightly doped (<0.06 e/C–H) samples and in photoconducting ones. In their famous theory Su, Schrieffer and Heeger (SSH) [1] attributed these features to spinless charged solitons as charge carriers. Their concept of solitons is based on the fact that *t*-PA exhibits two energetically degenerate groundstates, having different bond alternation phases A and B. With the help of the local displacements u_i at each site (projected on the polymer axis), phase A can be described by $u_i = (-1)^{i+1}u_0$ and phase B by $u_i = (-1)^i u_0$, where u_0 is the so-called dimerization. In fact u_0 is the bond alternation $R_> - R_<$ (larger and smaller C–C-bond lengths), projected on the polymer axis. The experimental value for u_0 is 0.026 Å (see [54, 55] for theoretical calculations and references to experiments therein). SSH introduced the staggered coordinates $\psi_i = (-1)^{i+1}u_i$, such that the bond alternation phase A can be described by $\psi_i = u_0$ and phase B by $\psi_i = -u_0$. The soliton is then the border between segments of the chain having different bond alternation phases. From SSH theory, which in principle is nothing but a Hückel model extended by a term describing the electron–phonon interaction, in the continuum limit it follows [1] that such a soliton centred at a site N_0 with a half-width L (in lattice sites) is described by a geometry (i denotes the lattice site)

$$\psi_i = u_0 \tanh[(N_0 - i)/L]. \tag{1}$$

From SSH theory in the continuum limit $L = 7$ can be derived. A brief explanation of the SSH model and of the method to compute dynamics from this model are given below, while the application of *ab initio* and PPP methods is described in [56–61], with special emphasis on the problem of spin contaminations in UHF (unrestricted Hartree–Fock) calculations.

The Su–Schrieffer–Heeger Hamiltonian (SSH) [1] is given by

$$\hat{H}' = \sum_n \left\{ [\beta_0 - (\hat{u}_n - \hat{u}_{n+1})\alpha] \sum_\sigma (\hat{c}^+_{n\sigma}\hat{c}_{n+1,\sigma} + \hat{c}^+_{n+1,\sigma}\hat{c}_{n\sigma}) + \frac{\hat{p}_n^2}{2M} + \frac{1}{2}K(\hat{u}_n - \hat{u}_{n+1})^2 - A(\hat{u}_n - \hat{u}_{n+1}) \right\}. \tag{2}$$

In (2) $\beta_0 = -2.5$ eV is the transfer or resonance integral between two neighbouring C–H groups; $\alpha = 4.8$ eV Å^{-1} is the electron–phonon coupling constant. The values of these constants [1] are determined such that an SSH (Hückel) calculation on an infinite, ordered and ideally dimerized chain results in a π-band width of 10 eV and a fundamental gap of roughly 2 eV. $M = 13\ m_p$ (in ordered chains) is the mass of a C–H unit, K is the spring constant due to the σ electrons between two neighbouring units. K and the linear potential constant A are determined such that the ideally dimerized chain shown in figure 1 represents the equilibrium geometry of the chain [26]. As shown in detail in appendix F of [71], in the adiabatic approximation the C–H units are considered as classical particles moving in the potential created by the π electrons and harmonic terms due to the σ electrons, which form a system of localized C–C bonds, underlying the delocalized π system.

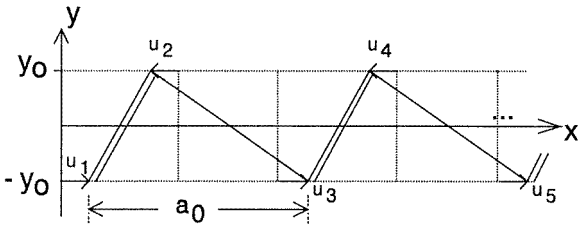

Figure 1. Sketch of the geometry and the coordinates we use for our simulations on *trans*-polyacetylene.

In figure 1, the u_n are the projections of the displacements of the C–H units from the equidistant chain onto the polymer axis, a_0 is the lattice constant of the equidistant chain and y_0 is the distance of the C–H units from the chain axis, which is kept constant in the SSH model. a_0 and y_0 are determined such that the long C–C bond in equilibrium has a length of 1.450 Å, that the short C–C bond has one of 1.366 Å and that the C–C–C angle has a value of 123.9°, a geometry which was obtained with the help of correlated *ab initio* calculations on the infinite chain by Suhai [62–65]. $\hat{u}_n$ is the operator of the displacements of the units parallel to the chain axis from their positions in the equidistant chain, and $\hat{p}_n$ the corresponding momentum operator. The operator $\hat{c}^+_{n\sigma}(\hat{c}_{n\sigma})$ creates (annihilates) an electron with spin orientation σ at unit n. The Fermi anti-commutation relations for these operators are obtained from,

$$\hat{c}^+|0\rangle = |1\rangle \qquad \hat{c}^+|1\rangle = 0 \qquad \hat{c}|0\rangle = 0 \qquad \hat{c}|1\rangle = |0\rangle \tag{3}$$

as

$$\{\hat{A}, \hat{B}\} \equiv \hat{A}\hat{B} + \hat{B}\hat{A}$$
$$\{\hat{c}_{n\sigma}, \hat{c}^+_{n'\sigma'}\} = \delta_{nn'}\delta_{\sigma\sigma'} \qquad \{\hat{c}_{n\sigma}, \hat{c}_{n'\sigma'}\} = \{\hat{c}^+_{n\sigma}, \hat{c}^+_{n'\sigma'}\} = 0. \tag{4}$$

2.2. Exact solution in the classical lattice limit

Exact solutions for the SSH Hamiltonian are not available. However, one can be derived in a special case, namely the limit of a completely classical lattice, i.e. replacing the momentum and displacement operators by real numbers. Since in Davydov soliton theory [66, 67] in proteins such a solution turned out to be extremely helpful, for example in judging the validity of temperature models, we want to give such an exact solution also for the SSH case.

With a classical lattice the SSH Hamiltonian is given by,

$$\hat{H} = \sum_j \hat{H}(j) + H_L(t)$$
$$\hat{H}(j) = \sum_n \{\beta_0 + \alpha[u_{n+1}(t) - u_n(t)](\hat{c}^+_{nj}\hat{c}_{n+1,j} + \hat{c}^+_{n+1,j}\hat{c}_{nj})\}$$
$$H_L(t) = \sum_n \left\{ \frac{p_n^2(t)}{2M} + \frac{K}{2}[u_{n+1}(t) - u_n(t)]^2 + A[u_{n+1}(t) - u_n(t)] \right\}. \qquad (5)$$

Note that an index in brackets, like (j), is an electron index, not an orbital index, and includes both spin orientations. The constants K and A are determined by a conventional SSH calculation as described in appendix F of [71]. The mass of a C–H unit M has to be determined in our eV ps^{-1} Å^{-1} system of units. For this Hamiltonian the time-dependent Schrödinger equation has to be solved,

$$\mathrm{i}\bar{h}\frac{\partial}{\partial t}|\psi\rangle = \hat{H}|\psi\rangle. \qquad (6)$$

Since $H_L(t)$ is a simple time-dependent real function we can write our state $|\psi\rangle$ as,

$$|\psi\rangle = \mathrm{e}^{-\mathrm{i}/\bar{h}G(t)}|\phi\rangle$$
$$G(t) \equiv \int_0^t H_L(t')\,\mathrm{d}t' \qquad \Rightarrow G(0) = 0$$
$$\Rightarrow \frac{\partial G(t)}{\partial t} = H_L(t). \qquad (7)$$

Insertion into the Schrödinger equation and multiplication of both sides with $\exp[(\mathrm{i}/\bar{h})G(t)]$ yields the equation for the electronic part of the state:

$$\mathrm{i}\bar{h}\frac{\partial}{\partial t}|\Phi\rangle = \sum_j \hat{H}(j)|\Phi\rangle \qquad |\psi\rangle = \chi(t)|\Phi\rangle$$
$$\chi(t) = \mathrm{e}^{-\mathrm{i}/\bar{h}G(t)} = \mathrm{e}^{-\mathrm{i}/\bar{h}\int_0^t H_L(t')\,\mathrm{d}t'}. \qquad (8)$$

For this electronic part we use as *ansatz* a Slater determinant built of ν one-particle states for ν electrons (note that in the one-particle SSH case a simple product of one-particle functions would yield the same results):

$$|\Phi\rangle = \frac{1}{\sqrt{\nu!}}\sum_P (-1)^p \hat{P}\prod_{j=1}^{\nu}|\varphi_j(j)\rangle. \qquad (9)$$

The symbols indicate that in each term of the determinant the sequence of orbitals $|\varphi_j\rangle$ in an individual product is always the same. The permutation operator P only changes the sequence of the electrons in their distribution among the orbitals. The two sides of the Schrödinger equation thus yield (electron index in brackets),

$$\mathrm{i}\bar{h}\frac{\partial}{\partial t}|\Phi\rangle = \frac{1}{\sqrt{\nu!}}\sum_P (-1)^p \hat{P}\sum_{j=1}^{\nu}\left[\mathrm{i}\bar{h}\frac{\partial}{\partial t}|\varphi_j(j)\rangle\right]\prod_{\substack{j'=1\\ j'\neq j}}^{\nu}|\varphi_{j'}(j')\rangle$$

$$\sum_j \hat{H}(j)|\Phi\rangle = \frac{1}{\sqrt{\nu!}} \sum_P (-1)^p \hat{P} \sum_{j=1}^{\nu} [\hat{H}(j)|\varphi_j(j)\rangle] \prod_{\substack{j'=1 \\ j'\neq j}}^{\nu} |\varphi_{j'}(j')\rangle$$

$$\Rightarrow \frac{1}{\sqrt{\nu!}} \sum_P (-1)^p \hat{P} \sum_{j=1}^{\nu} \left[\mathrm{i}\hbar \frac{\partial}{\partial t} - \hat{H}(j) \right] |\varphi_j(j)\rangle \prod_{\substack{j'=1 \\ j'\neq j}}^{\nu} |\varphi_{j'}(j')\rangle = 0. \tag{10}$$

The last equation can only be solved if,

$$\mathrm{i}\hbar \frac{\partial}{\partial t}|\varphi_j(k)\rangle = \hat{H}(k)|\varphi_j(k)\rangle \tag{11}$$

for all occupied (others do not exist here) orbitals j and all electrons k, or without loss of generality,

$$\mathrm{i}\hbar \frac{\partial}{\partial t}|\varphi_j\rangle = \hat{H}_j|\varphi_j\rangle$$
$$\hat{H}_j = \sum_n \{\beta_0 + \alpha[u_{n+1}(t) - u_n(t)](\hat{c}^+_{nj}\hat{c}_{n+1,j} + \hat{c}^+_{n+1,j}\hat{c}_{nj})\} \tag{12}$$

where the creation (annihilation) operators create (annihilate) an electron in spin orbital j at site n and obey the usual anti-commutation relations for fermions. This equation can be solved by expansion in a series of basis states at sites n:

$$|\varphi_j\rangle = \sum_n c_{nj}(t)\hat{c}^+_{nj}|0\rangle. \tag{13}$$

Using the anti-commutation relations we obtain,

$$\hat{H}_j|\varphi_j\rangle = \sum_n \{[\beta_0 + \alpha(u_{n+1}(t) - u_n(t))]c_{n+1,j}(t) + [\beta_0 + \alpha(u_n(t) - u_{n-1}(t))]c_{n-1,j}(t)\}\hat{c}^+_{nj}|0\rangle$$

$$\mathrm{i}\hbar \frac{\partial}{\partial t}|\varphi_j\rangle = \sum_n \dot{c}_{nj}(t)\hat{c}^+_{nj}|0\rangle. \tag{14}$$

Thus our *ansatz* solved the Schrödinger equation exactly if the time dependent coefficients obey,

$$\mathrm{i}\hbar \dot{c}_{nj} = \beta_n(t)c_{n+1,j} + \beta_{n-1}(t)c_{n-1,j}$$
$$\beta_n(t) = \beta_0 + \alpha_n(t) \qquad \alpha_n(t) = \alpha[u_{n+1}(t) - u_n(t)]. \tag{15}$$

Note that we use open chains, i.e., we assume implicitly that for $n = N$ the first term on the right-hand side is not present, while for $n = 1$ the second term vanishes. Now we can compute a Hamiltonian function $H(t)$:

$$H(t) = \langle\psi|\hat{H}|\psi\rangle = \langle\psi|\sum_j \hat{H}_j|\psi\rangle + \langle\psi \mid \psi\rangle H_L(t). \tag{16}$$

From the equations for the $c_{nj}(t)$ it can be easily shown that they are norm conserving, i.e., $\langle\psi(t) \mid \psi(t)\rangle = \langle\psi(0) \mid \psi(0)\rangle = 1$ if the wave function is initially normalized. Further, it can be shown that the equations are overlap conserving, i.e. $\langle\varphi_j(t) \mid \varphi_{j'}(t)\rangle = \langle\varphi_j(0) \mid \varphi_{j'}(0)\rangle = \delta_{jj'}$ if the orbitals are initially orthonormal. Thus,

$$H(t) = \chi(t)\chi^*(t)\sum_j \langle\varphi_j|\hat{H}_j|\varphi_j\rangle + H_L(t) = \sum_j \langle\varphi_j|\hat{H}_j|\varphi_j\rangle + H_L(t). \tag{17}$$

The first term follows from the Slater–Condon rules for expectation values of a one-particle Hamiltonian between two identical Slater determinants built from orthonormal spin orbitals. Until now summations over j were running over all spin orbitals. However, since electrons

of opposite spins always occupy the same spatial orbital, we can sum from now on over orbitals and multiply the respective term with an occupation number o_j (0, 1 or 2):

$$H(t) = \sum_j o_j \langle \varphi_j | \hat{H}_j | \varphi_j \rangle + H_L(t). \tag{18}$$

Evaluation of the expectation values and definition of the density matrix,

$$P_{nm} \equiv \sum_j o_j c_{nj} c^*_{mj} \tag{19}$$

yields,

$$H(t) = \sum_n [\beta_n P_{n+1,n} + \beta_{n-1} P_{n-1,n}] + H_L(t). \tag{20}$$

Now with the help of Hamilton's equations we obtain the equations of motion for the lattice:

$$\dot{p}_n = -\frac{\partial H(t)}{\partial u_n} \qquad \dot{u}_n = \frac{\partial H(t)}{\partial p_n} = \frac{p_n}{M}$$

$$\dot{p}_n = 2\alpha\{\mathrm{Re}\,[P_{n,n+1}](1-\delta_{nN}) - \mathrm{Re}\,[P_{n,n-1}](1-\delta_{n1})\} - \frac{\partial H_L(t)}{\partial u_n}. \tag{21}$$

Differentiation of the lattice Hamiltonian yields our final set of equations,

$$\begin{aligned}
\dot{p}_n &= 2\alpha\{\mathrm{Re}\,[P_{n,n+1}](1-\delta_{nN}) - \mathrm{Re}\,[P_{n,n-1}](1-\delta_{n1})\} \\
&\quad + K[(u_{n+1}-u_n)(1-\delta_{nN}) + (u_{n-1}-u_n)(1-\delta_{n1})] + A(\delta_{n1}-\delta_{nN}) \\
\dot{u}_n &= p_n/M \\
\mathrm{i}\hbar\dot{c}_{nj} &= \sum_{nn'} h_{nn'} c_{n'j}
\end{aligned} \tag{22}$$

where,

$$\begin{aligned}
h_{nn'}(t) &= \beta_{nn'} + \alpha_{nn'}(t) \\
\beta_{nn'} &= \beta_0[\delta_{n',n+1}(1-\delta_{nN}) + \delta_{n',n-1}(1-\delta_{n1})] \\
\alpha_{nn'}(t) &= \alpha_n(t)\delta_{n',n+1}(1-\delta_{nN}) + \alpha_{n-1}(t)\delta_{n',n-1}(1-\delta_{n1}) \\
\alpha_n(t) &= \alpha[u_{n+1}(t) - u_n(t)].
\end{aligned} \tag{23}$$

The actual procedure we use for the numerical solution of these equations is given in appendix G of [71]. Since we have a Hamiltonian system at $T = 0$ K with a time independent Hamiltonian operator it can be easily shown that the total energy is a conserved quantity (for $T = 0$ K). The total state vector is,

$$|\psi\rangle = \chi(t)\frac{1}{\sqrt{\nu!}}\sum_P (-1)^p \hat{P} \prod_{j=1}^{\nu} \left[\sum_n c_{nj}(t)\hat{c}^+_{nj}|0\rangle \right]. \tag{24}$$

Note, that the result is identical to the result from the so-called $|\Phi_2\rangle$ *ansatz* [71] state (see the appendix for details), besides a time-dependent phase factor which is unimportant for conventional expectation values, but important if spectra should be computed. The completely adiabatic model would be obtained if we assumed the eigenvectors and eigenvalues for the description of the electrons to be constant during a time step.

Note that in the limit of short times the lattice can be assumed to be slow as compared to the electrons. Thus one can set the time derivative of the lattice momenta equal to zero and insert the resulting relations for the lattice displacements into the equations for the

electrons. In this way one obtains a set of coupled discrete nonlinear Schrödinger equations (DNLS) for the electrons:

$$i\hbar\dot{c}_{nj} = \beta(c_{n+1,j} + c_{n-1,j}) - \frac{2\alpha^2}{K}\sum_{j'} o_{j'}\{\mathrm{Re}\,[c_{nj'}c^*_{n+1,j'}]c_{n+1,j} - \mathrm{Re}\,[c_{nj'}c^*_{n-1,j'}]c_{n-1,j}\}. \quad (25)$$

Interestingly, this set of equations is mathematically identical to the corresponding DNLS which can be obtained in Davydov theory for the dynamics of amide-I vibrations in proteins coupled to the lattice, provided that more than one vibrational quantum is studied. However, there the physical meaning of the variables and parameters is a different one.

2.3. The adiabatic treatment

Since the adiabatic treatment of the dynamics is documented in the original papers by SSH [1] as well as in appendix F of our paper [71] we do not want to repeat the equations here. It is enough to mention that in this case the electrons are considered to be fast enough to follow the lattice dynamics instantaneously. Thus at each time step the Hamiltonian matrix is formed from the respective geometry of the chain and diagonalized. From the molecular orbital (MO) coefficients obtained in this way the gradient of the electronic energy with respect to the lattice geometry can be computed analytically. With the help of these gradients the lattice geometry for the next time step is calculated. Note that this procedure is computationally much less demanding than our method which follows the electron dynamics explicitly. However, the simple diagonalization of the electronic Hamiltonian matrix at each time step yields MO coefficients with an undefined phase, i.e. given an MO to any one of the eigenvalues of the Hamiltonian, then the same MO multiplied with any arbitrary phase factor also solves the Hamiltonian with the same eigenvalue. This implies that the adiabatic procedure is unable to yield the time development of the phase factors of the electronic wave functions. These phases, however, are of extreme importance if the calculation of spectra from the dynamics is desired as we show below.

2.4. Vibrational spectra

We want to conclude this section by showing how vibrational spectra can be calculated from dynamic simulations. The procedure we are using at present is based on Heller's [68] method, which consists of the transformation of a delta-function in the frequency domain into the time domain, and the application of closure properties of the states of a system. The absorption cross section is given by,

$$\sigma(\omega) - \omega\int_0^\infty \mathrm{Re}\,[\mathrm{e}^{\mathrm{i}/\hbar(E_i+\hbar\omega)t}S(t)]\,\mathrm{d}t \quad (26)$$

where E_i simply sets the energy scale, i.e., if we perform an excited state simulation in the SSH model and the excitation energy E_i (i for initial) is simply the difference of the energy levels between which the initial vertical excitation takes place. $S(t)$ is the autocorrelation function,

$$S(t) = \langle\psi(0) \mid \psi(t)\rangle \quad (27)$$

which in our case is given by,

$$S(t) = \mathrm{e}^{-\mathrm{i}/\hbar\int_0^t H_L(t')\,\mathrm{d}t'}\langle\Delta(0) \mid \Delta(t)\rangle$$
$$|\Delta(t)\rangle = \frac{1}{\sqrt{\nu!}}\sum_p (-1)^p\hat{P}\prod_{j=1}^{\nu}|\varphi_j(t)\rangle. \quad (28)$$

The overlap between the two Slater determinants can be formulated as the determinant of a matrix $\mathbf{S}(t)$ which, however, has to be formed from spin orbitals not from orbitals. This is most easily verified by computing explicitly the overlap between two 2×2 or 3×3 Slater determinants. The matrix $\mathbf{S}(t)$ is defined by its elements. Thus we obtain,

$$\begin{aligned} S(t) &= \chi(t) \det \mathbf{S}(t) \\ S_{ij}(t) &= \langle \varphi_i(0) \mid \varphi_j(t) \rangle = \sum_n c^*_{ni}(0) c_{nj}(t) \\ \chi(t) &= \mathrm{e}^{-\mathrm{i}/\hbar \int_0^t H_L(t')\,\mathrm{d}t'} \\ H_L(t) &= \sum_n \left[\frac{p_n^2}{2M} + \frac{K}{2}(u_{n+1} - u_n)^2 + A(u_{n+1} - u_n) \right]. \end{aligned} \tag{29}$$

Currently we are using this formalism to compute photoinduced vibrational spectra from excited state dynamics. It is completely obvious that for the calculation of the matrix elements $S_{ij}(t)$ the time dependence of the phases of the MOs is of utmost importance, which cannot be obtained with an adiabatic treatment or density matrix methods.

Further, with the SSH Hamiltonian for the calculation of the dynamics, we used the geometries obtained as functions of time in PPP/MP2 (many-body perturbation theory of second order in Moeller–Plesset partitioning) calculations to calculate the electronic spectra with the help of the random phase approximation. These were averaged over time to obtain spectra comparable to experiment. The results are the subject of another paper [69].

3. Results and discussion

3.1. Temperature dependence calculated with our exact solution

Temperature is included in our treatment via Langevin equations (see appendix F of [71]) for the lattice. Since Langevin equations are strictly correct only for classical systems, our results for very low temperature ($T = 10$ K) are approximative. We had to use a very small time step size of 0.01 fs, because the electron dynamics are much faster than the lattice dynamics. In previous, adiabatic simulations it was always assumed, that the electrons follow the lattice motions instantaneously, thus a time step of 1 to 1.25 fs was sufficient. Since in our study we want to simulate results including electron–electron interactions (Pariser–Parr–Pople, PPP model) accurately as possible with our exact SSH solution, we have to choose $\beta_0 = -2.5$ eV and $\alpha = 4.8$ eV Å^{-1}. The value of u_0 has to be chosen such that it is smaller than the experimental one, because from PPP and MINDO (all-valence-electron semiempirical method) calculations it is known that the soliton width L is roughly equal to three lattice sites. However, the SSH Hamiltonian with experimental u_0 values gives soliton half-widths around seven lattice sites. To obtain the desired soliton width of three sites, we used $u_0 = 0.1$ Å. We placed initially a soliton of tanh shape with $L = 3$ and centred at $N_0 = 26$ in a neutral chain of 51 units. The initial values for the c_{nj} were obtained from a conventional static SSH calculation on the system with our initial geometry (optimized neutral soliton geometry in the centre of the chain). Then we performed time simulations using the above-derived formalism at different temperatures, namely $T = 0$, 10, 50 and 100 K. The algorithm for the solution of the electronic part of the equations of motion is described in some detail in appendix G of [71], while the time evolution of the lattice coordinates was calculated with a simple one-step procedure. In some of the calculations we used two different time step sizes, namely 0.01 fs (200 000 time steps) and 0.001 fs (2 000 000 time steps), respectively. In the latter calculations the input and calculated

parameters were: chain length $N = 51$, resonance integral $\beta_0 = -2.5$ eV, electron–phonon coupling strength $\alpha = 4.8$ eV Å^{-1}, equilibrium dimerization $u_0 = 0.1$ Å, spring constants for the C–C σ bonds $K = 16.9539$ eV Å^{-2}, linear potential term $A = -5.676\,88$ eV Å^{-1}, time constant of the heat bath $\Gamma = 1.095\,63$ ps^{-1} and half width of the Gaussian distribution for the random forces $\sigma = 2.562\,33$ (eV Å^{-1})^2 (10 K). Figure 2 shows the kinetic energy of the lattice (solid lines) together with the error in total energy (dashed lines) as a function of time for a time step of 0.01 fs (left panel) and for a time step of 0.001 fs (right panel) at $T = 0$ K. From the figure it is completely obvious that in case of the larger time step size the error in total energy is increasing with time, and one could assume that the larger time step is not well suited for our investigation. However, if we look at the time evolution of the α-spin density as function of site and time (in figure 3) we see that the picture is completely the same in both calculations (thus we show only one of them). Since the chain geometry is optimized, the only (fast) change in the course of time is in the phase of the electronic wave function. As figure 4 indicates, also the geometry as a function of site and time is identical for the two time step sizes.

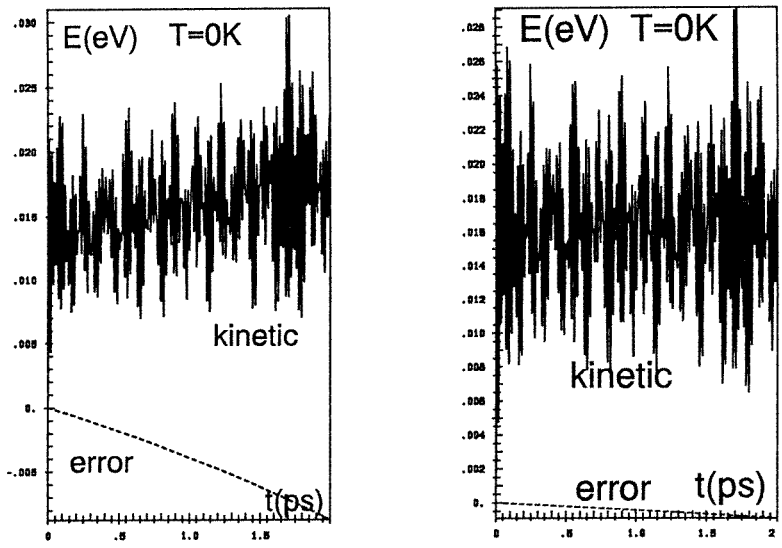

Figure 2. Kinetic energy of the lattice (solid lines) together with the error in total energy (dashed lines) as functions of time for a time step of 0.01 fs (left panel) and for a time step of 0.001 fs (right panel) at $T = 0$ K.

However, to be sure that we can use the larger time step we performed a comparative investigation with both time step sizes also at a temperature of 50 K, since the small changes in the course of time at 0 K might give misleading results. In figure 5 we show again the energies in the same way as above but now for $T = 50$ K. It is obvious that the differences between the two time step sizes are not very pronounced in this case again. In figure 6 we display the quantity $A(t)$, which is the time average of the lattice kinetic energy up to time t divided by $(N-1)kT/2$ (k is Boltzmann's constant). When the system is in thermal equilibrium this value should approach unity. Our results show that within the simulation time we just drive the system into thermal equilibrium, where the approach of $A(t)$ to unity is somewhat better in the case with the smaller time step size. However, the differences

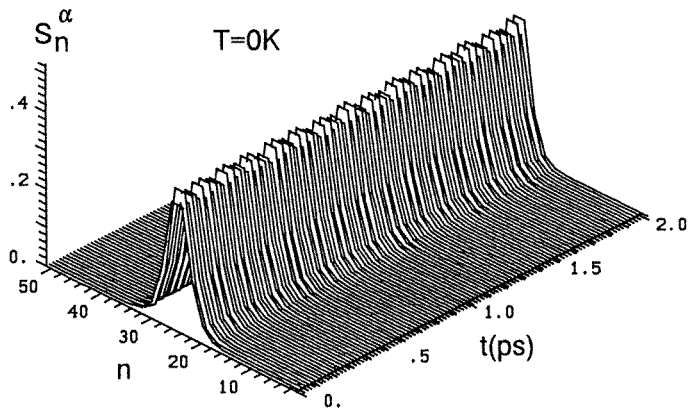

Figure 3. α-spin density as function of time t and site n for our model as described in the text, calculated with a time step of 0.01 fs.

in $A(t)$ are not very pronounced in the two cases and therefore can serve as a further indication that we can safely use the larger time step size and thus save a considerable amount of computer time.

More interesting than these quantities would be definitely the coordinates as a function of time; however, in such a plot one does not see too much because the thermal fluctuations in the coordinates completely cover up the soliton movement. However, we can plot again the spin density as a function of time and site for the two cases, which is done in figure 7. Here at first sight the results look completely different for the two time step sizes. However, a closer look at the two plots reveals clearly that the mobility of the soliton is the same in both cases, but the restricted movement occurs in the lower panel to the other side of the chain and somewhat later, which is not a basic differences for our qualitative conclusions. Therefore we decided to perform the other two simulations at 10 and 100 K with the larger time step due to the tremendous amount of computation time necessary for the smaller one. In figure 8 we show the energetics and $A(t)$ for the case of 10 K, while figure 9 shows the corresponding spin density. We see from figure 8 that $A(t)$ does not approach exactly unity, which, in our opinion, indicates that the use of the Langevin model at low temperatures such as 10 K is somewhat problematic; however, the overshooting of $A(t)$ over unity is not tremendous. The spin densities shown in figure 9 indicate clearly that some very small shifts in the soliton position occur just as the experimental results suggest: soliton mobility is changing gradually from immobile to free movement between 10 and 100 K. Now as a last step we have to examine the results for 100 K which are shown in figures 10 and 11. Obviously $A(t)$ approaches again a value slightly larger than unity. However, we have seen from the $T = 50$ K case that this might be a consequence of the time step size, while it does not affect other quantities like the spin densities which are the important ones. Figures 10 and 11 indicate clearly that the soliton is freely mobile at $T = 100$ K. The thermal fluctuations excite the soliton initially at rest to a moving one which crosses the complete chain within the simulation time. This behaviour of our model with increasing temperature is in complete agreement with experiment [1], and shows that besides its simplicity the model seems to be rather close to reality. However, if quantities like electronic excitation spectra should be computed we admit that our simple essentially Hückel type model must be augmented by electron–electron interaction and consequently correlation corrections have to be included in the one-particle picture. However, we discuss

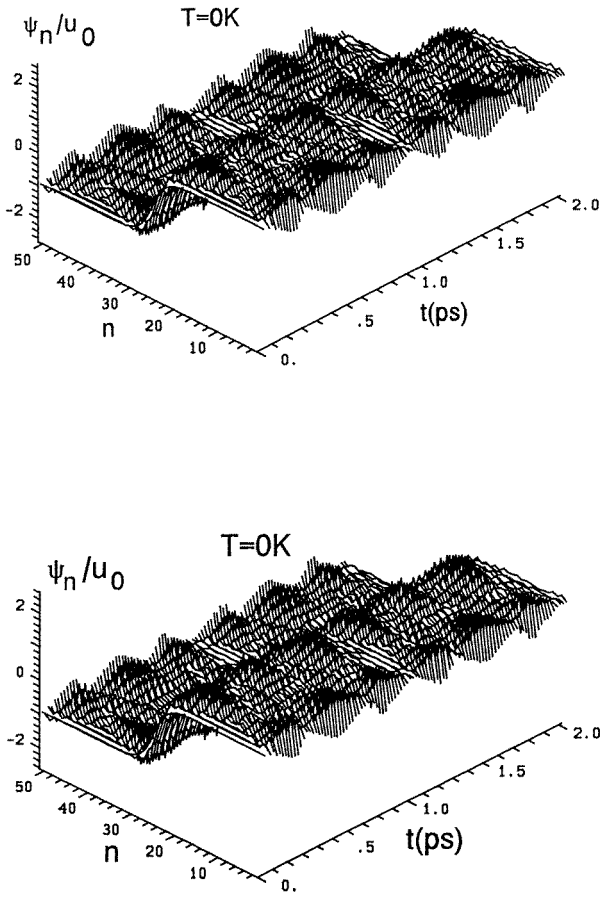

Figure 4. Time evolution of the staggered lattice coordinates divided by the equilibrium dimerization as a function of lattice site for the model as described in the text at $T = 0$ K for a time step of 0.01 fs (upper panel) and 0.001 fs (lower panel).

these issues in another publication [69]. The corresponding results at 100 K, but calculated with the smaller time step size for 2 ps simulation time (calculated on the IBM Risc) we do not show here. In this case within the simulation time of 2 ps $A(t)$ does not even reach unity. Again the onset of soliton motion is delayed, as observed also in the 50 K case. However, here the onset of motion does not even occur within the simulation time of 2 ps. However, with the help of an ALPHA Station 500/333 MHz workstation from Digital which performs much better than the IBM Risc used for all calculations described above we could perform a calculation for $T = 100$ K through a larger simulation time. The IBM Risc needed, as mentioned, 725 CPU hours calculation time for 1 ps simulation time, while the ALPHA Station uses only 100 CPU hours for the same 1 ps simulation time. The results of a 4 ps calculation (18.4 CPU days on the ALPHA Station) at $T = 100$ K are shown in figures 12 and 13. The results indicate clearly that after a longer simulation time first of all $A(t)$ reaches a value slightly larger than 1. Note that $A(t)$ reaches unity exactly only in a completely classical Langevin system where all fluctuations in kinetic energy are fully at random. Since our system is not entirely classical and there exists a non-random part of

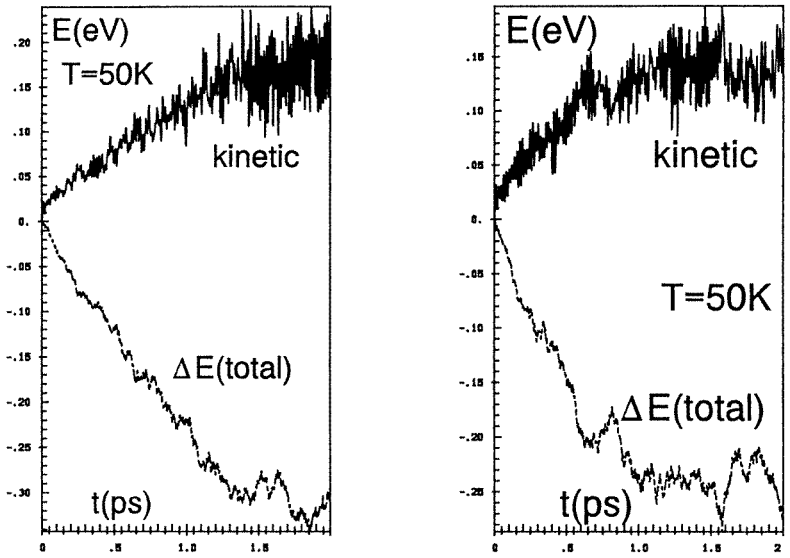

Figure 5. Kinetic energy of the lattice (solid lines) together with the change in total energy due to temperature effects (ΔE; dashed lines) as functions of time for a time step of 0.01 fs (left panel) and for a time step of 0.001 fs (right panel) at $T = 50$ K.

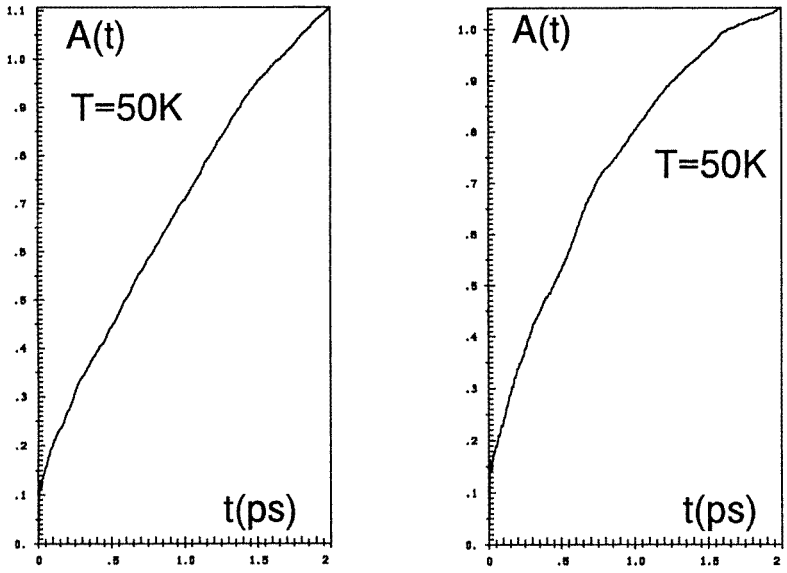

Figure 6. The quantity $A(t)$, which is the time average of the lattice kinetic energy up to time t divided by $(N-1)kT/2$ (k is Boltzmann's constant) for $T = 50$ K as a function of time, using a time step of 0.01 fs (left panel) and one of 0.001 fs (right panel).

the kinetic energy after the soliton starts to move (due to its motion) $A(t)$ can be expected to end up around unity but not exactly at $A = 1$. Secondly, the soliton starts to become completely mobile after about 3 ps. The mobility is indicated by the fact that the soliton is able to reach the chain end completely at 100 K, while it became stuck before the actual

chain end in the 50 K simulation. We only want to mention here, in order to indicate the correctness of our programs, that during the first 2 ps simulation time on the ALPHA Station we obtained the same results as on the IBM Risc. We want to point out the fact that within our model the qualitative conclusions about the mobility of the neutral soliton as function of temperature remain the same for the two time step sizes considered. The only difference is the larger delay time until soliton motion sets in in the case of the smaller time step size and the different directions of the soliton motion. However, since temperature effects are described by random forces and a dissipation term, the latter difference is not surprising or of physical importance. Since the system is symmetric with respect to the centre of the chain, no direction of soliton movement is physically preferred. Only the motion as such is of importance and can be measured. The longer delay time of soliton movement also is of no importance, since the system anyway has to be given time for thermal equilibration before conclusions can be drawn. The final conclusion from the discussed set of calculations is that starting from 10 K the soliton mobility gradually increases and from 100 K the soliton is completely mobile, only restricted by the limited chain length. This agrees completely with the results of DNP (dynamic nuclear polarization) experiments (see [1] and references therein). Note that vibrational spectra could be calculated from the simulations presented in this work if one used the formalism presented in 2.4

3.2. Temperature dependence calculated with the adiabatic model

In the adiabatic model we have the advantage that the calculations are much less demanding with regard to computation time. However, the adiabatic model, as mentioned above, has the drawback that the time dependent phases at the molecular orbitals cannot be calculated, and thus vibrational spectra as described in 2.4 cannot be obtained from adiabatic dynamics. We want to present briefly the results of our adiabatic simulations here as well, because it might be possible that the mobility of the solitons could be described equally well with both methods, ours and the adiabatic one. Temperature effects are included in the adiabatic calculations in the same way as in our model, namely by the introduction of random forces and dissipation in the lattice equations. Thus the values of the parameters are the same as in the previous calculations. Only the half-width of the Gaussian distribution for the random forces, σ, depends on the size of the time step. Thus for time steps of 0.01 fs and 0.001 fs σ has the same values as stated in the last paragraph. For the time steps of $\tau = 1$ fs, 0.1 fs, 0.01 fs, 0.001 fs and temperatures $T = 10$ K, 50 K, 100 K the half-widths are given by

$$\sigma = 2.562\,33 \times 10^{-4} \frac{\text{fs}}{\text{K}} \frac{T}{\tau} \left(\frac{\text{eV}}{\text{Å}} \right)^2 . \tag{30}$$

In figure 14 we show the energetics of the simulations, especially the error in total energy at $T = 0$ K to get a feeling for what time step size is necessary in the adiabatic case to obtain correct results. Obviously, in agreement with previous experience, already for a time step of 1 fs the error in the total energy is sufficiently small in an adiabatic simulation to obtain reliable results, despite the simple one-step procedure used in the time simulation. For the smaller time steps the error is reduced drastically. However, the time evolution of the α-spin density for the different temperatures and time steps as shown in figure 15 indicates clearly that in the adiabatic model even the qualitative results concerning the mobility of the solitons as function of temperature do not show a consistent change when the time step size is reduced (we show only the cases with $T = 10$ and 100 K; the 50 K case shows a similar inconclusive behaviour). Even with the smallest time step we see that the mobility at lower temperatures is overestimated, although less pronounced than for

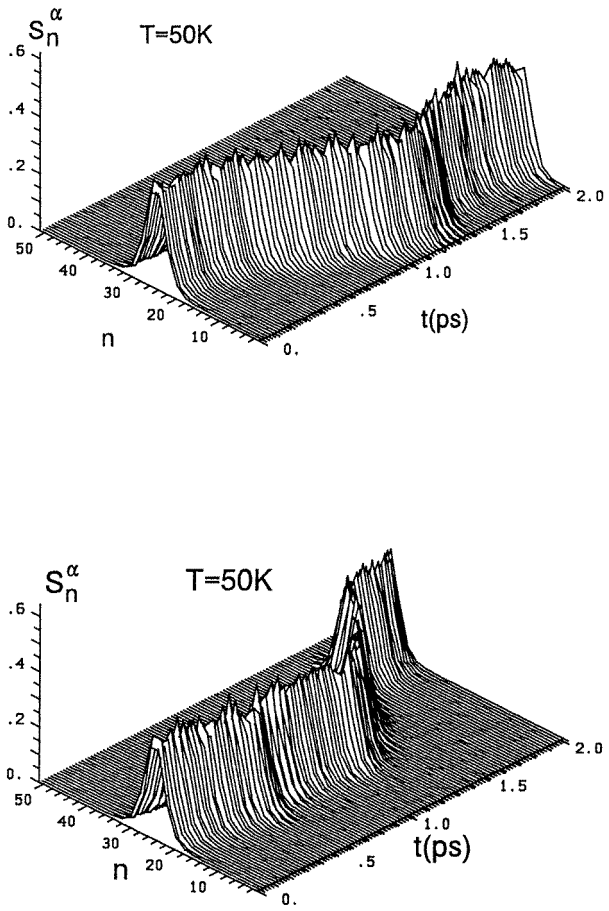

Figure 7. α-spin density as a function of time t and site n for our model as described, calculated with time steps of 0.01 fs (upper panel) and 0.001 fs (lower panel).

the larger ones. However, for even smaller time steps (necessary here to obtain consistent results, while with our model, as we have seen above, already a time step of 0.01 fs would be sufficient) one would have to think about using a larger numerical precision than in all our calculations (double precision: 64 bits per word) and then the calculations would become even more demanding than in those for our model. Thus we have to conclude from these results that the adiabatic model, although it saves a tremendous amount of computation time (in comparative calculations using the two models with the same time step size) is not able to reproduce the experimental facts on soliton mobility with a reasonable time step size. Thus in addition to the problem that the adiabatic model is unable to produce the time dependence of the phases at the molecular orbitals, it could yield also misleading results about the dynamics of the solitons as function of temperature.

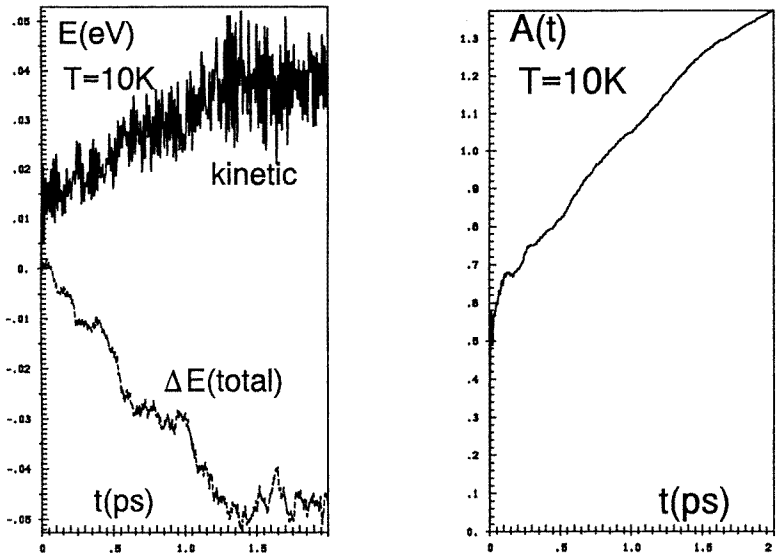

Figure 8. Kinetic energy of the lattice (solid line) together with the change in total energy due to temperature effects (ΔE; dashed line) as functions of time (left panel) and the quantity $A(t)$, which is the time average of the lattice kinetic energy up to time t divided by $(N-1)kT/2$ (k is Boltzmann's constant) for $T = 10$ K as a function of time (right panel), using a time step of 0.01 fs.

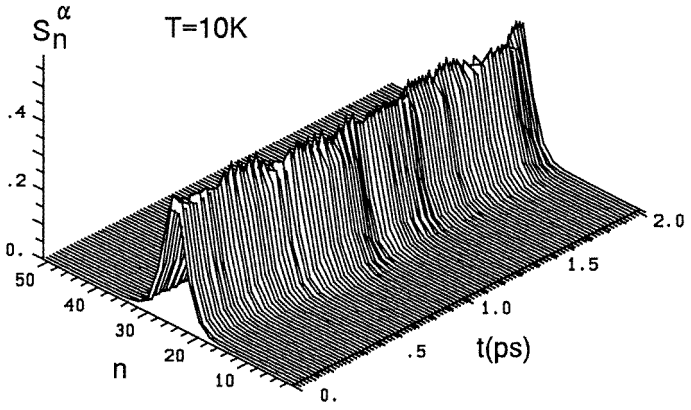

Figure 9. α-spin density as a function of time t and site n for our model as described in the text, calculated with a time step of 0.01 fs at 10 K.

4. Conclusion

The discussion given above clearly indicates that our method is able to reproduce experimentally known facts about soliton mobility as function of temperature in *trans*-polyacetylene. However, what this discussion also shows clearly is that these calculations need a tremendous amount of computation time, also because we need to do all the calculations in double precision (64 bits per word). We have performed them on an IBM RISC 6000 320H (25 MHz) workstation and a calculation with a time step of 0.001 fs over 2 ps needed 86 990 CPU minutes (=1450 CPU hours = 60.4 CPU days), while the

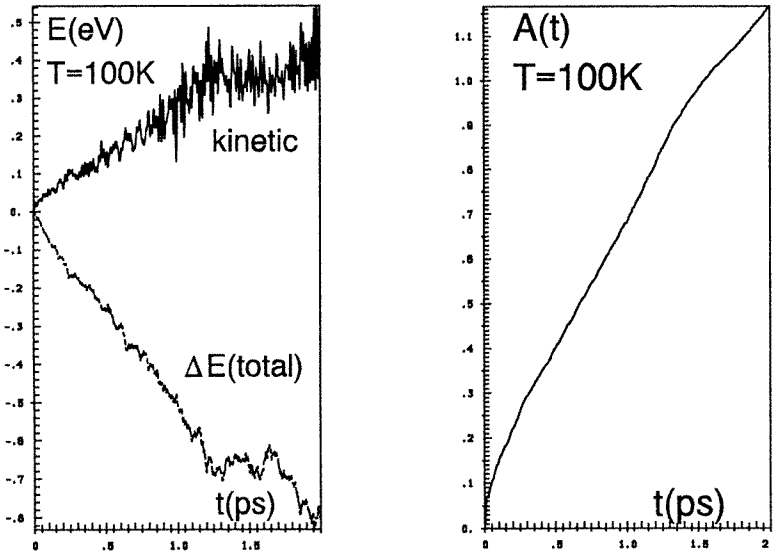

Figure 10. Kinetic energy of the lattice (solid line) together with the change in total energy due to temperature effects (ΔE; dashed line) as functions of time (left panel) and the quantity $A(t)$, which is the time average of the lattice kinetic energy up to time t divided by $(N-1)kT/2$ (k is Boltzmann's constant) for $T = 100$ K as a function of time (right panel), using a time step of 0.01 fs.

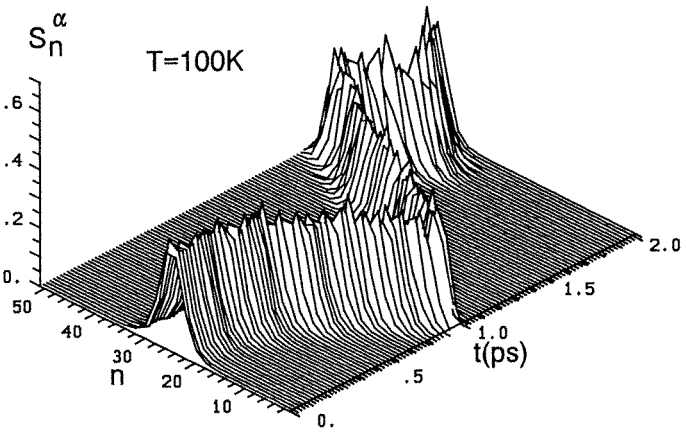

Figure 11. α-spin density as a function of time t and site n for our model as described in the text, calculated with a time step of 0.01 fs at 100 K.

calculation with the larger time step of 0.01 fs required a tenth of that time, still about 6 days of pure CPU time. We found, on the other hand, that an ALPHA Station 500/333 MHz is by roughly a factor of seven faster than the IBM Risc and enabled us to carry out the calculation for 100 K and the smaller time step for a simulation time of 4 ps. Further we have found that the adiabatic model, which is widely in use and much less tedious to calculate numerically, is not able to reproduce the experimental facts on the dynamics as a function of temperature correctly with reasonable time step sizes (0.001 fs is still not sufficiently small). On the contrary, the results obtained with the adiabatic model change

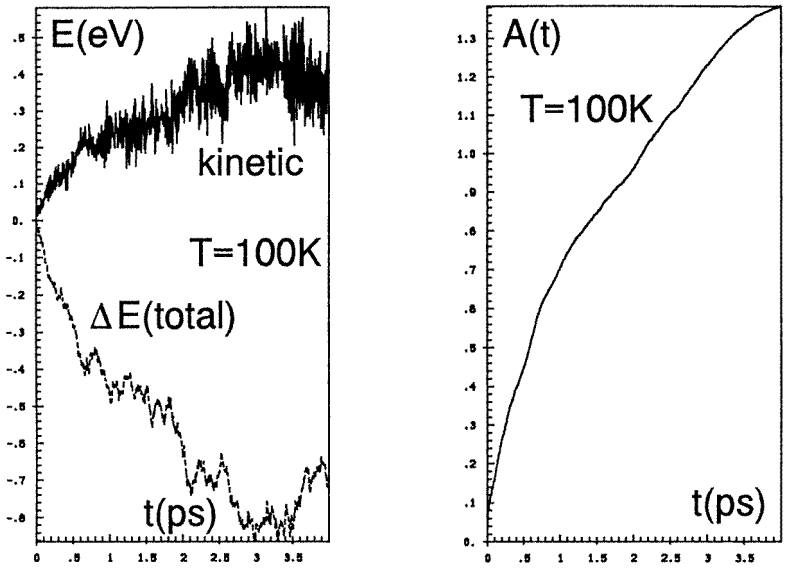

Figure 12. Kinetic energy of the lattice (solid line) together with the change in total energy due to thermal effects (ΔE; dashed line) as functions of time (left panel) and the quantity $A(t)$, which is the time average of the lattice kinetic energy up to time t divided by $(N-1)kT/2$ (k is Boltzmann's constant) for $T = 100$ K as a function of time (right panel), using a time step of 0.001 fs for a simulation time of 4 ps calculated with an ALPHA Station.

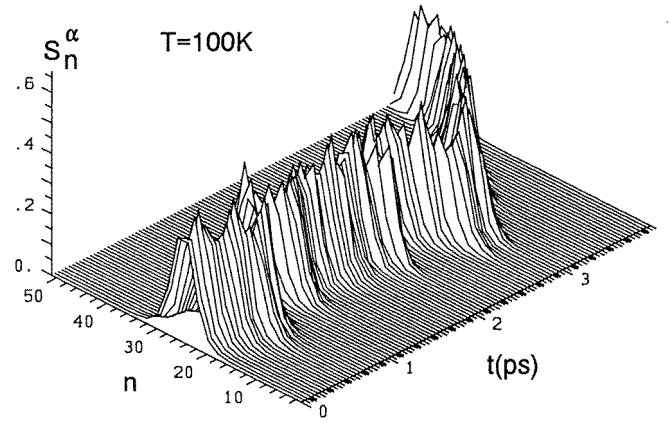

Figure 13. α-spin density as a function of time t and site n for our model as described in the text, calculated with a time step of 0.001 fs at 100 K (4 ps calculation done on an ALPHA Station).

even qualitatively when the time step is reduced. Further, neither the adiabatic model nor a density matrix method as described in [70] are able to yield the time dependence of the phases at the electronic wave functions, while our model yields it automatically. These phases are of utmost importance for the calculation of spectra as we outlined in section 2.4. The so-called $|\Phi_2\rangle$ state (which is based on Davydov's $|D_2\rangle$ state *ansatz* for high-frequency oscillations coupled to lattice phonons) as defined in [71] is derived in detail in appendix A. A comparison shows that it yields the same time evolution of the lattice and of the electron

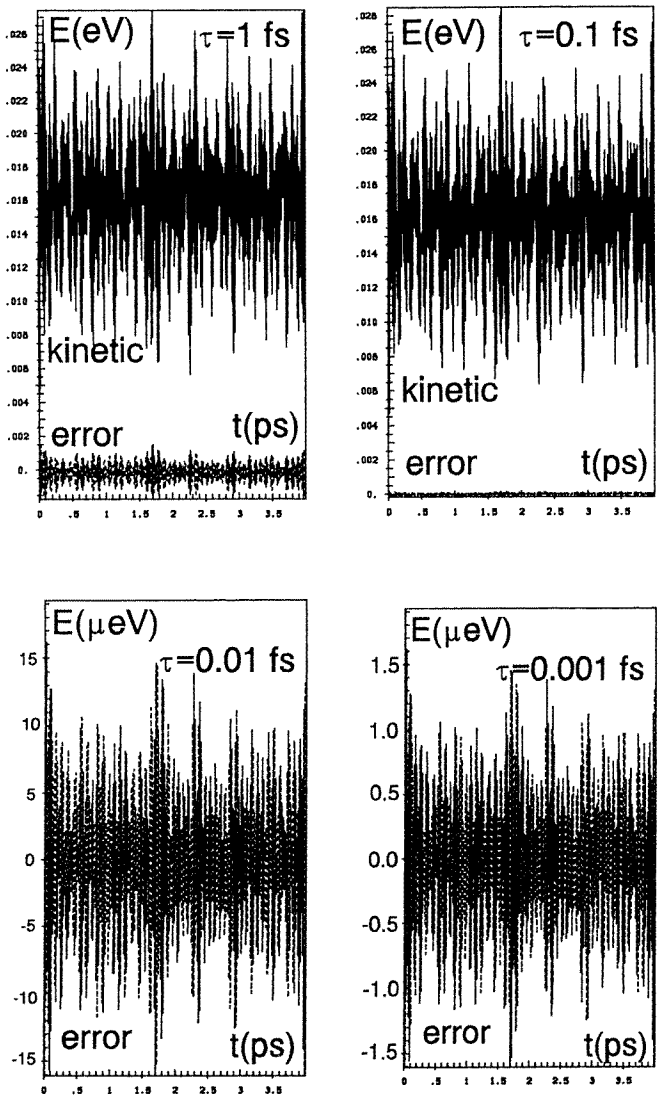

Figure 14. Kinetic energy of the lattice (solid lines, only for two time steps sizes τ) together with the error in total energy for $T = 0$ K (ΔE; dashed lines) as functions of time, using time steps of $\tau = 1$ fs, 0.1 fs, 0.01 fs and 0.001 fs, calculated with the adiabatic model.

distribution as the exact classical solution, however, with different phases. Therefore this state can be called a semi-classical one. Note that such findings are also of a more general importance, because a similar type of state is widely used in Davydov soliton theory where a similar discussion on exact special case solutions can be found in the literature [66, 67].

One could assume that a simple calculation of the potential energy of a chain as a function of the displacement of the centre of a soliton might yield a good estimate of its mobility. Thus we performed such calculations and in figure 16 we plot this potential energy in units of K (kelvin) as a function of the position of the soliton centre for two different values of u_0. Figure 16(a) indicates that for displacements of the soliton centre around the

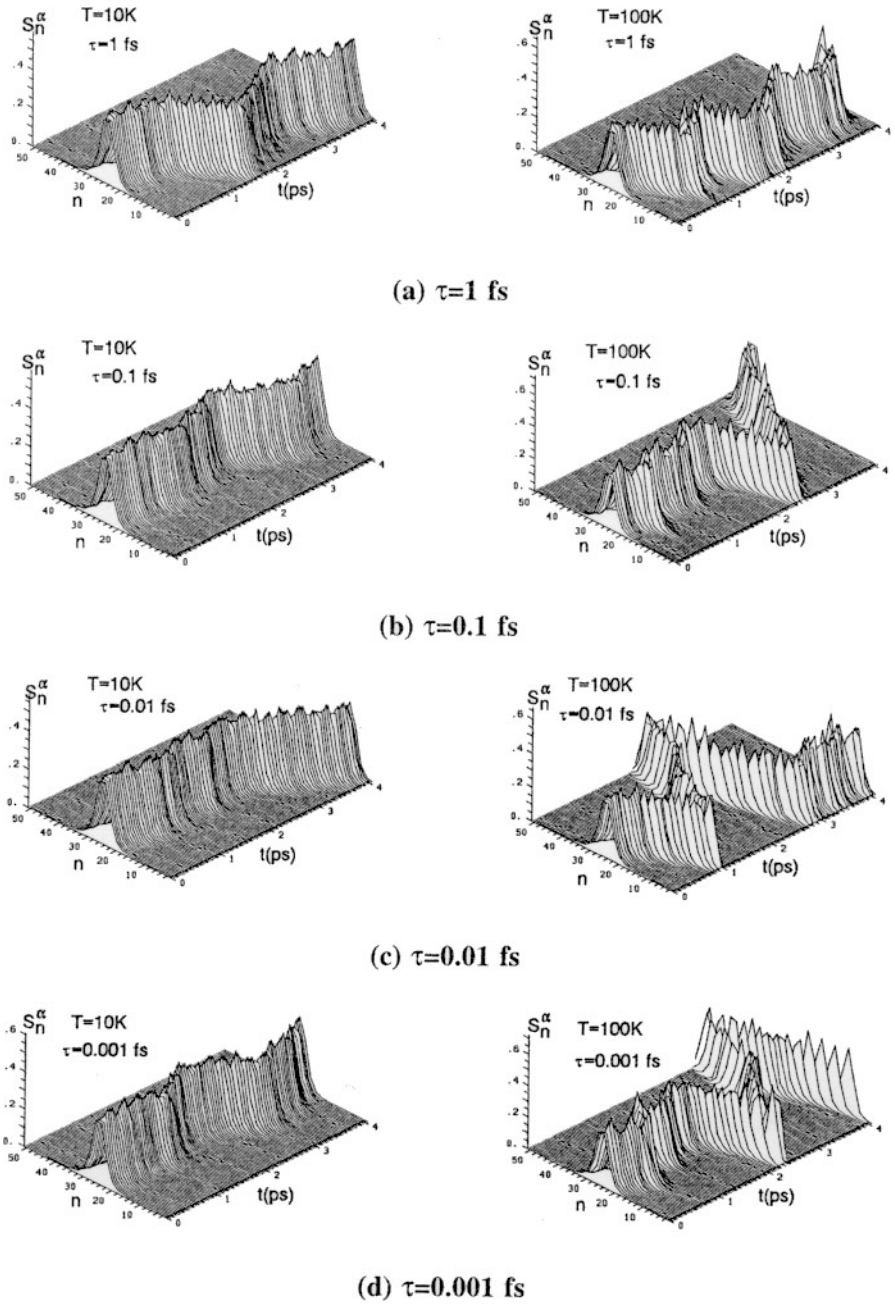

Figure 15. α-spin density as a function of time t and site n for the adiabatic model as described in the text, calculated with four different time step sizes of (a) $\tau = 1$ fs, (b) $\tau = 0.1$ fs, (c) $\tau = 0.01$ fs and (d) $\tau = 0.001$ fs, at the temperatures $T = 10$ and $T = 100$ K.

centre of the chain only a negligible amount of energy is needed. However, since the forces acting on the lattice due to temperature do not act in a coherent way but, rather, introduce some disorder even in a small region around the chain centre they cannot drive the soliton out of its equilibrium position. The disorder introduced by temperature thus should have as

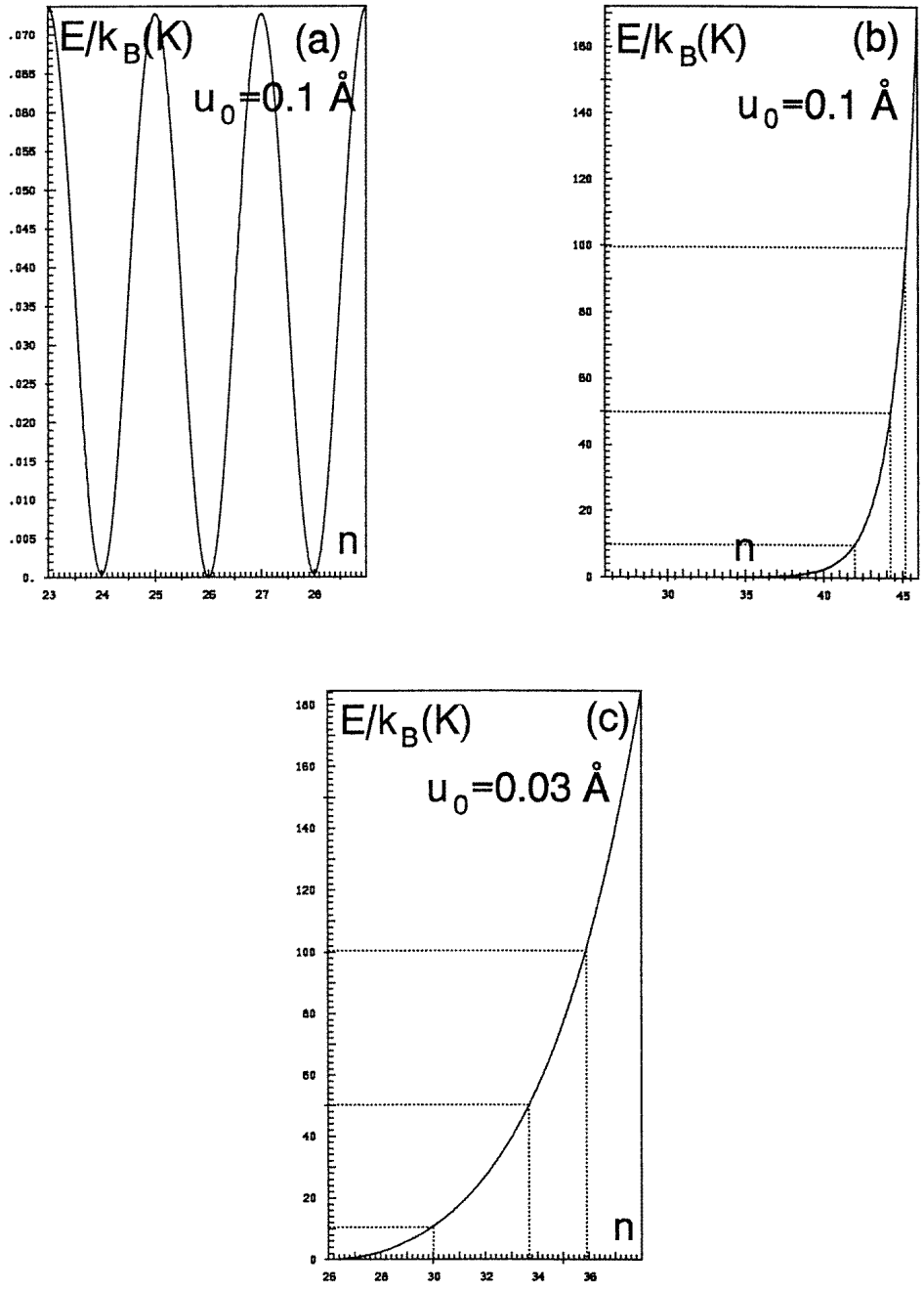

Figure 16. The potential energy E/k_B (k_B is Boltzmann's constant) in K (kelvin) as a function of the position n (in lattice sites) of the centre of a soliton of the form $u_i = (-1)^{i+1}u_0 \tanh[(n-i)/L]$ (half-width L given in lattice sites) in a chain of 51 units for (K and A optimized for the respectively ideally dimerized chains) (a) $u_0 = 0.1$ Å; $L = 3$; small region around the centre of the chain ($K = 16.9539$ eV Å^{-2}), (b) $u_0 = 0.1$ Å; $L = 3$ ($K = 16.9539$ eV Å^{-2}, $A = -5.676\,88$ eV Å^{-1}), (c) $u_0 = 0.03$ Å; $L = 7$ ($K = 27.9580$ eV Å^{-2}, $A = -6.073\,16$ eV Å^{-1}).

usual (Anderson localization) a localizing effect on the soliton. In figure 16(b) we show the potential energy for larger distances of the soliton from the centre of the chain (site 26). The dotted lines are drawn to guide the eye for the three temperatures considered by us. What has to be noted is first of all that for an energy of 100 K the soliton mobility is somewhat underestimated, because the potential barrier of 100 K corresponds just to a movement from the centre of the chain up to site 45, while our simulations indicate that at 100 K the soliton is able to reach the chain end (site 51). Further, a barrier of 10 K corresponds to a displacement of the soliton to site 42, while clearly from our simulations as well as from experiments we know that the soliton is still more or less immobile at this temperature. At the intermediate value of the potential barrier of 50 K, the soliton mobility from such an estimate would be more or less the same as for 100 K, which again overestimates it, a behaviour which also shows up in simulation with the adiabatic model. In figure 16(c) we show the corresponding potential for $u_0 = 0.03$ Å, which is closer to the experimental one. Here the situation is similar; however, now the overestimation of the mobility at 50 K is reduced. From the plot one could estimate a mobility threshold at about 20 K in this case, as reported earlier by Su *et al* [1]. In conclusion it seems to us that only our model yields the correct estimate for soliton mobility, while the adiabatic one overestimates it at lower temperatures.

Acknowledgments

Major parts of the derivations presented in this work have been completed during a stay of the author at the Center for Theoretical Studies of Physical Systems at Clark Atlanta University, Atlanta, GA in April 1996. The author wants to thank all members of the Center for their kind hospitality, especially Professors C Handy and A Z Msezane who also made his stay at the Center possible. The kind support and help obtained by the author from Professor A R Al-Arfaj, Chairman of the Chemistry Department at the King Fahd University of Petroleum and Minerals in Dhahran, and all members of the Department is gratefully acknowledged. Last but not least the author wants to thank Dr W Utz for his invaluable help with the calculation on the ALPHA Station in Erlangen.

Appendix A. Connection with $|\Phi_2\rangle$ state

For the discussion of the $|\Phi_2\rangle$ *ansatz* state we have to rewrite first of all the SSH Hamiltonian into a more familiar form by introduction of the usual creation and annihilation operators for the lattice phonons which are of the same form as in the case of the Davydov Hamiltonian and obey Bose commutation relations:

$$[\hat{A}, \hat{B}] \equiv \hat{A}\hat{B} - \hat{B}\hat{A}$$
$$[\hat{b}_k, \hat{b}^+_{k'}] = \delta_{kk'} \qquad [\hat{b}^+_k, \hat{b}^+_{k'}] = [\hat{b}_k, \hat{b}_{k'}] = 0. \tag{A1}$$

For this purpose we rewrite first the Hamiltonian to get rid of the linear terms leading to [71]

$$\hat{H}' = \sum_n \{[\beta - (\hat{q}_n - \hat{q}_{n+1})\alpha] \sum_\sigma (\hat{c}^+_{n\sigma}\hat{c}_{n+1,\sigma} + \hat{c}^+_{n+1,\sigma}\hat{c}_{n\sigma}) + \frac{\hat{p}_n^2}{2M} + \frac{1}{2}K(\hat{q}_n - \hat{q}_{n+1})^2\} + C$$

$$q_n(t) = u_n(t) + \left[n - \frac{1}{2}(N+1)\right]\frac{A}{K} - \frac{1}{N}\sum_m u_m(t=0)$$

$$C = -(N-1)\frac{A^2}{2K} \qquad \beta = \beta_0 - \frac{A}{K}\alpha \tag{A2}$$

where N is the number of sites in a chain. The $\hat{q}_n$ are displacement operators relative to the minimum geometry of the lattice potential in (2). The one-electron SSH Hamiltonian is then given as

$$\hat{H}' = \sum_{n\sigma}\left[\beta + \sum_k \hbar\omega_k B_{nk}(\hat{b}_k + \hat{b}_k^+)\right](\hat{c}_{n\sigma}^+\hat{c}_{n+1,\sigma} + \hat{c}_{n+1,\sigma}^+\hat{c}_{n\sigma}) + \sum_k \hbar\omega_k\left(\hat{b}_k^+\hat{b}_k + \frac{1}{2}\right) + C. \tag{A3}$$

Separation of the constant term leads to

$$\hat{H}' = \hat{H} + D \qquad D = \frac{1}{2}\sum_k \hbar\omega_k + C \tag{A4}$$

and the gauge transformation

$$|\Psi\rangle = \mathrm{e}^{-\mathrm{i}/\hbar(\frac{1}{2}\sum_k \hbar\omega_k + C)t}|\Phi\rangle = \mathrm{e}^{-\mathrm{i}/\hbar Dt}|\Phi\rangle. \tag{A5}$$

Therefore

$$\mathrm{i}\hbar\frac{\partial}{\partial t}|\Phi\rangle = \hat{H}|\Phi\rangle \tag{A6}$$

with

$$\hat{H} = \sum_{n\sigma}\left[\beta + \sum_k \hbar\omega_k B_{nk}(\hat{b}_k + \hat{b}_k^+)\right](\hat{c}_{n\sigma}^+\hat{c}_{n+1,\sigma} + \hat{c}_{n+1,\sigma}^+\hat{c}_{n\sigma}) + \sum_k \hbar\omega_k \hat{b}_k^+\hat{b}_k \tag{A7}$$

where $\mathbf{B}$ is given by

$$B_{nk} = \frac{\alpha}{\omega_k}\sqrt{\frac{1}{2\hbar\omega_k M}}(V_{n+1,k} - V_{nk}) \tag{A8}$$

ω_k being the eigenfrequencies and $\boldsymbol{V}_k$ the coefficient vector of the normal mode k of the decoupled ($\alpha = 0$) lattice, i.e. they are the solutions of the eigenvalue problem

$$\frac{1}{M}\mathbf{K}\boldsymbol{V}_k = \omega_k^2\boldsymbol{V}_k$$
$$K_{nm} = K[2(1 - \tfrac{1}{2}\delta_{n1} - \tfrac{1}{2}\delta_{nN})\delta_{nm} - \delta_{m,n-1}(1-\delta_{n1}) - \delta_{m,n+1}(1-\delta_{nN})]. \tag{A9}$$

The translation mode ($\omega = 0$) has to be excluded from the summations. The operators are defined by

$$\hat{q}_n = \sum_k \sqrt{\frac{\hbar}{2M\omega_k}}V_{nk}(\hat{b}_k^+ + \hat{b}_k)$$
$$\hat{p}_n = \mathrm{i}\sum_k \sqrt{\frac{M\hbar\omega_k}{2}}V_{nk}(\hat{b}_k^+ - \hat{b}_k). \tag{A10}$$

As in the so-called $|\mathrm{D}_2\rangle$ *ansatz* for the treatment of Davydov soliton dynamics we can start in our case from the $|\Phi_0\rangle$ state (a more general state including quantum effects in the lattice, which is discussed in detail in [71]) and drop the site and orbital indices at the coherent state amplitudes. Note that in one-electron theories as used here it makes no difference in the results whether we use a Slater determinant or a simple product built from

one-electron states. Therefore as *ansatz* for the total wave function $|\Phi\rangle$ we use the simple product of the electronic wave function with a common coherent phonon state $|\beta\rangle$:

$$|\Phi\rangle = \frac{1}{\sqrt{\nu!}}\sum_P (-1)^P \hat{P}\left[\prod_{j=1}^{\nu}|\varphi_j(j)\rangle\right]|\beta\rangle$$
$$|\varphi_j\rangle = \sum_n c_{nj}(t)\hat{c}_{nj}^+|0\rangle_e$$
$$|\beta\rangle = \exp\left\{\sum_k [b_k(t)\hat{b}_k^+ - b_k^*(t)\hat{b}_k]\right\}|0\rangle_p. \tag{A11}$$

Here the MO coefficients $c_{nj}(t)$ and the coherent state amplitudes $b_k(t)$ are the unknown time dependent variables. As before the b_k are defined with respect to the deviations q_n from the equilibrium geometry of the lattice (see appendix A of [71]). With this *ansatz* the lattice is treated semi-classically, but one obtains explicit equations of motion for the MO coefficients of the electrons, in contrast to the adiabatic treatment, where the electrons are assumed to follow the ions instantaneously. We start from the Lagrangian built with the *ansatz* given in (A11) (where j runs from here on over the spatial orbitals only unless otherwise mentioned, and o_j is an occupation number):

$$L = \frac{\mathrm{i}\overline{h}}{2}\sum_{nj} o_j(\dot{c}_{nj}c_{nj}^* - \dot{c}_{nj}^* c_{nj})X_j + \frac{\mathrm{i}\overline{h}}{2}\sum_k (\dot{b}_k b_k^* - \dot{b}_k^* b_k)X$$
$$- \sum_n \left\{\left[\beta + \sum_k \overline{h}\omega_k B_{nk}(b_k^* + b_k)\right]\sum_j o_j c_{n+1,j}c_{nj}^*\right.$$
$$\left. + \left[\beta + \sum_k \overline{h}\omega_k B_{n-1,k}(b_k^* + b_k)\right]\sum_j o_j c_{n-1,j}c_{nj}^*\right\}X_j - \sum_k \overline{h}\omega_k |b_k|^2 X \tag{A12}$$

where X and X_j are given by

$$X = \prod_j \left(\sum_n |c_{nj}|^2\right)^{o_j} \qquad X_j = \prod_{j'}\left(\sum_n |c_{nj'}|^2\right)^{o_{j'}-\delta_{jj'}} = \frac{X}{N_j}$$
$$N_j = \sum_n |c_{nj}|^2. \tag{A13}$$

These terms as well as the norm N_j are constant in time as we will prove below.

Differentiation of L with X and X_j considered as variables as given in (A13) yields together with

$$\frac{\partial X}{\partial c_{nj}^*} = o_j c_{nj}\prod_{j'}\left(\sum_m |c_{mj'}|^2\right)^{o_{j'}-\delta_{jj'}} = o_j c_{nj}X_j$$
$$\frac{\partial X_{j'}}{\partial c_{nj}^*} = (o_j - \delta_{jj'})c_{nj}\prod_{j''}\left(\sum_m |c_{mj''}|^2\right)^{o_{j''}-\delta_{j'j''}-\delta_{jj''}} = (o_j - \delta_{jj'})c_{nj}X_{jj'} \tag{A14}$$

the following terms:

$$\frac{\mathrm{d}}{\mathrm{d}t}\frac{\partial L}{\partial \dot{c}_{nj}^*} = -\frac{\mathrm{i}\overline{h}}{2}[o_j\dot{c}_{nj}X_j + o_j c_{nj}X_j]$$
$$\frac{\partial L}{\partial \dot{c}_{nj}^*} = \frac{\mathrm{i}\overline{h}}{2}\left\{o_j\dot{c}_{nj}X_j + \sum_{mj'} o_{j'}(\dot{c}_{mj'}c_{mj'}^* - \dot{c}_{mj'}^* c_{mj'})(o_j - \delta_{jj'})c_{nj}\frac{X_j}{N_{j'}}\right\}$$

$$+o_j c_{nj}\left[\frac{\mathrm{i}\bar{h}}{2}\sum_k(\dot{b}_k b_k^* - \dot{b}_k^* b_k) - \sum_k \bar{h}\omega_k |b_k|^2\right]X_j - A_j o_j c_{nj}\dot{X}_j$$
$$-A_n o_j c_{n+1,j}X_j - A_{n-1}o_j c_{n-1,j}X_j \tag{A15}$$

where

$$A_j \equiv \sum_{mj'}\frac{A_m}{N_{j'}}(c_{m+1,j'}c_{mj'}^* + c_{m+1,j'}^* c_{mj'})(o_{j'} - \delta_{jj'}) = A_j^*$$
$$\text{since } \frac{o_{j'}}{o_j}(o_j - \delta_{jj'}) = (o_{j'} - \delta_{jj'})$$
$$A_n \equiv \left[\beta + \sum_k \bar{h}\omega_k B_{nk}(b_k^* + b_k)\right] = A_n^*. \tag{A16}$$

Therefore we obtain as equation of motion

$$\mathrm{i}\bar{h}o_j\dot{c}_{nj}X_j = -\frac{\mathrm{i}\bar{h}}{2}o_j c_{nj}\dot{X}_j + C_j o_j c_{nj}X_j + A_n o_j c_{n+1,j}X_j + A_{n-1}o_j c_{n-1,j}X_j \tag{A17}$$

with the abbreviations

$$C_j = A_j - \frac{\mathrm{i}\bar{h}}{2}\sum_{mj'}\frac{1}{N_{j'}}(\dot{c}_{mj'}c_{mj'}^* - \dot{c}_{mj'}^* c_{mj'})(o_{j'} - \delta_{jj'}) - \frac{\mathrm{i}\bar{h}}{2}\sum_k(\dot{b}_k b_k^* - \dot{b}_k^* b_k)$$
$$+\sum_k \bar{h}\omega_k |b_k|^2 = C_j^*$$
$$X_{jj'} = \frac{X_j}{N_{j'}} = \frac{X_{j'}}{N_j} \qquad N_j X_j = X. \tag{A18}$$

Thus we obtain finally

$$\mathrm{i}\bar{h}\dot{c}_{nj} = -\frac{\mathrm{i}\bar{h}}{2}c_{nj}\frac{\dot{X}_j}{X_j} + C_j c_{nj} + A_n c_{n+1,j} + A_{n-1}c_{n-1,j}. \tag{A19}$$

The time derivative of the norm is

$$\mathrm{i}\bar{h}\dot{N}_j = \sum_n[(\mathrm{i}\bar{h}\dot{c}_{nj})c_{nj}^* - (-\mathrm{i}\bar{h}\dot{c}_{nj}^*)c_{nj}]. \tag{A20}$$

Substitution of (A19) and its complex conjugate into (A20) yields (note that C_j and A_n are real numbers)

$$\mathrm{i}\bar{h}\dot{N}_j = -\frac{\mathrm{i}\bar{h}}{2}N_j\frac{\dot{X}_j}{X_j} + C_j N_j + \sum_n[A_n c_{n+1,j} + A_{n-1}c_{n-1,j}]c_{nj}^*$$
$$-\left[\frac{\mathrm{i}\bar{h}}{2}N_j\frac{\dot{X}_j}{X_j} + C_j N_j + \sum_n[A_n c_{n+1,j}^* + A_{n-1}c_{n-1,j}^*]c_{nj}\right] = -\mathrm{i}\bar{h}N_j\frac{\dot{X}_j}{X_j}. \tag{A21}$$

The second equality holds, because

$$\sum_{n=1}^{N-1}A_n c_{n+1,j}^* c_{nj} = \sum_{n=2}^{N}A_{n-1}c_{nj}^* c_{n-1,j}$$
$$\sum_{n=2}^{N}A_{n-1}c_{n-1,j}^* c_{nj} = \sum_{n=1}^{N-1}A_n c_{nj}^* c_{n+1,j}. \tag{A22}$$

Thus we arrive at

$$\dot{N}_j = -N_j\frac{\dot{X}_j}{X_j} \Rightarrow \dot{N}_j X_j + N_j\dot{X}_j = \frac{\mathrm{d}}{\mathrm{d}t}(N_j X_j) = \frac{\mathrm{d}}{\mathrm{d}t}\left(\prod_j N_j^{o_j}\right) = \dot{X} = 0$$

$$X(t) = X(t=0) = 1. \tag{A23}$$

From this result follows

$$0 = \frac{\mathrm{d}}{\mathrm{d}t}\left(\prod_j N_j^{o_j}\right) = \sum_j o_j \dot{N}_j \left(\prod_{j'} N_{j'}^{o_{j'}-\delta_{jj'}}\right) = \sum_j o_j \dot{N}_j X_j \Rightarrow \sum_j o_j N_j \dot{X}_j = 0. \tag{A24}$$

Further we can rewrite our equations of motion to

$$\begin{aligned} \mathrm{i}\bar{h}\dot{c}_{nj} &= -\frac{\mathrm{i}\bar{h}}{2}\frac{\dot{X}_j}{X_j}c_{nj} + C_j(t)c_{nj} + \sum_m g_{nm}(t)c_{mj} \\ g_{nm}(t) &= A_n(t)\delta_{m,n+1}(1-\delta_{nN}) + A_{n-1}(t)\delta_{m,n-1}(1-\delta_{n1}). \end{aligned} \tag{A25}$$

With this form of the equations we can show now that not only the product of the norms of all orbitals, but also the norm of every individual orbital remains constant. This is most easily done by performing the phase transformation

$$c_{nj} = d_{nj}\exp\left[-\frac{\mathrm{i}}{\bar{h}}\int_0^t C_j(t')\,\mathrm{d}t'\right] \tag{A26}$$

leading to

$$\mathrm{i}\bar{h}\dot{d}_{nj} = -\frac{\mathrm{i}\bar{h}}{2}\frac{\dot{X}_j}{X_j}d_{nj} + \sum_m g_{nm}(t)d_{mj} = \frac{\mathrm{i}\bar{h}}{2}\frac{\dot{N}_j}{N_j}d_{nj} + \sum_m g_{nm}(t)d_{mj}. \tag{A27}$$

Therefore now each of our spin orbitals carried a phase

$$|\varphi_j\rangle = \sum_n c_{nj}(t)\hat{c}_{nj}^+|0\rangle_e = \mathrm{e}^{-\mathrm{i}/\bar{h}\int_0^t C_j(t')\,\mathrm{d}t'}\sum_n d_{nj}(t)\hat{c}_{nj}^+|0\rangle_e. \tag{A28}$$

Since the total wave function is a linear combination of products of all occupied orbitals, we have in spin orbital notation

$$|\Phi\rangle = \frac{1}{\sqrt{\nu!}}\sum_P (-1)^p \hat{P}\prod_{j=1}^{\nu}\left[\mathrm{e}^{-\mathrm{i}/\bar{h}\int_0^t C_j(t')\,\mathrm{d}t'}\sum_n d_{nj}(t)\hat{c}_{nj}^+|0\rangle_e\right]|\beta(t)\rangle \tag{A29}$$

where here j runs over the occupied spin orbitals only. The total phase factor γ resulting from the above transformation thus is given by

$$\gamma = \prod_j [\mathrm{e}^{-\mathrm{i}/\bar{h}\int_0^t C_j(t')\,\mathrm{d}t'}]^{o_j} = \prod_j [\mathrm{e}^{-\mathrm{i}/\bar{h}\int_0^t o_j C_j(t')\,\mathrm{d}t'}] = \mathrm{e}^{-\mathrm{i}/\bar{h}\int_0^t o_j C_j(t')\,\mathrm{d}t'} \tag{A30}$$

where here j runs over the occupied spatial orbitals again. Now the integrand in this phase factor can be computed in a rather simple way. The equations of motion (A25) yield

$$\begin{aligned} \mathrm{i}\bar{h}\dot{c}_{nj}c_{nj}^* &= -\frac{\mathrm{i}\bar{h}}{2}\frac{\dot{X}_j}{X_j}|c_{nj}|^2 + C_j|c_{nj}|^2 + \sum_m g_{nm}c_{mj}c_{nj}^* \\ -\mathrm{i}\bar{h}\dot{c}_{nj}^*c_{nj} &= \frac{\mathrm{i}\bar{h}}{2}\frac{\dot{X}_j}{X_j}|c_{nj}|^2 + C_j|c_{nj}|^2 + \sum_m g_{nm}^*c_{mj}^*c_{nj}. \end{aligned} \tag{A31}$$

When we add these two equations and divide by 2, we obtain

$$\frac{\mathrm{i}\bar{h}}{2}(\dot{c}_{nj}c_{nj}^* - \dot{c}_{nj}^*c_{nj}) = C_j|c_{nj}|^2 + \frac{1}{2}\sum_m (g_{nm}c_{mj}c_{nj}^* + g_{nm}^*c_{mj}^*c_{nj}). \tag{A32}$$

With g_{nm} as defined in (A25) we can write

$$\frac{\mathrm{i}\bar{h}}{2}(\dot{c}_{nj}c_{nj}^* - \dot{c}_{nj}^*c_{nj}) = C_j|c_{nj}|^2 + A_n(c_{n+1,j}c_{nj}^* + c_{n+1,j}^*c_{nj}) \tag{A33}$$

and therefore

$$\frac{i\hbar}{2}\sum_{nj'}\frac{1}{N_{j'}}(\dot{c}_{nj'}c^*_{nj'}-\dot{c}^*_{nj'}c_{nj'})(o_{j'}-\delta_{jj'})$$
$$=\sum_{nj'}\frac{1}{N_{j'}}[C_{j'}|c_{nj'}|^2+A_n(c_{n+1,j'}c^*_{nj'}+c^*_{n+1,j'}c_{nj'})](o_{j'}-\delta_{jj'})$$
$$=\sum_{j'}(o_{j'}-\delta_{jj'})C_{j'}+A_j \tag{A34}$$

where we used (A16) and the definition of the norm which is $\sum_n |c_{nj}(t)|^2 = N_j(t)$. Thus insertion of the above result into (A18) yields

$$C_j=-\sum_{j'}(o_{j'}-\delta_{jj'})C_{j'}-\frac{i\hbar}{2}\sum_k(\dot{b}_k b^*_k-\dot{b}^*_k b_k)+\sum_k\hbar\omega_k|b_k|^2 \tag{A35}$$

and therefore the integrand in the total phase factor γ is

$$\sum_j o_j C_j=-\frac{i\hbar}{2}\sum_k(\dot{b}_k b^*_k-\dot{b}^*_k b_k)+\sum_k\hbar\omega_k|b_k|^2. \tag{A36}$$

Now we have, if the $\boldsymbol{d}_j$ are orthonormal, i.e. $\boldsymbol{d}_i^+\boldsymbol{d}_j=\delta_{ij}$ holds:

$$c_{nj}(t)=e^{i\gamma_j(t)}d_{nj}(t)\qquad \gamma_j(t)\equiv-\frac{1}{\hbar}\int_0^t C_j(t')\,dt'$$
$$\Rightarrow S_{ij}=\sum_n c_{ni}c^*_{nj}=e^{i(\gamma_j(t)-\gamma_i(t))}\sum_n d_{ni}d^*_{nj}=e^{i(\gamma_j(t)-\gamma_i(t))}\delta_{ij}=\delta_{ij}. \tag{A37}$$

Therefore we must seek solutions of the system of equations

$$i\hbar\dot{d}_{nj}-\sum_n g_{nm}d_{mj}=\frac{i\hbar}{2}\frac{\dot{N}_j}{N_j}d_{nj}\qquad N_j=\sum_n d^*_{nj}d_{nj}. \tag{A38}$$

For this purpose we solve the corresponding equations with vanishing right-hand side

$$i\hbar\dot{d}_{nj}-\sum_n g_{nm}d_{nj}=0. \tag{A39}$$

Having a solution $d_{nj}(t)$ of (A39) we compute the time derivative of the norm $N_j(t)$ of this solution:

$$i\hbar\dot{N}_j(t)=\sum_n[(i\hbar\dot{d}_{nj}(t))d^*_{nj}(t)-(-i\hbar\dot{d}^*_{nj}(t))d_{nj}(t)]. \tag{A40}$$

Substitution of (A39) into (A40) leads to

$$i\hbar\dot{N}_j(t)=\sum_{nm}[g_{nm}(t)d_{mj}(t)d^*_{nj}(t)-g^*_{nm}(t)d^*_{mj}(t)d_{nj}(t)]$$
$$=\sum_{nm}[g_{nm}(t)-g^*_{mn}(t)]d^*_{mj}(t)d^*_{nj}(t). \tag{A41}$$

Thus, if the matrix $\mathbf{g}(t)$ is Hermitian we obtain $N_j(t)=1$ (for $N_j(t=0)=1$, as is the case) for the solution of (A39). Then, since $dN_j(t)/dt=0$, our solution of (A39) is also solution of (A38), which we are looking for, with a conserved norm. For the matrix $\mathbf{g}(t)$ we have from (A25) together with (A16)

$$g_{nm}(t)=A_n(t)\delta_{m,n+1}(1-\delta_{nN})+A_{n-1}(t)\delta_{m,n-1}(1-\delta_{n1})$$
$$A_n(t)=\left\{\beta+\sum_k\hbar\omega_k B_{nk}[b^*_k(t)+b_k(t)]\right\}=A^*_n(t)$$

$$\Rightarrow g_{n,n+1} = A_n \qquad g_{n+1,n} = \sum_m g_{m,m-1}\delta_{m,n+1} = \sum_m A_{m-1}\delta_{m,n+1} = A_n = g_{n,n+1}$$

$$g_{n-1,n} = \sum_m g_{m,m+1}\delta_{m,n-1} = \sum_m A_m \delta_{m,n-1} = A_{n-1} = g_{n,n-1}$$

$$\Rightarrow \mathbf{g}(t) = \mathbf{g}^+(t) \tag{A42}$$

and thus $\mathbf{g}(t)$ is Hermitian, and solutions of (A39) are also solutions of (A38). Thus for the derivation of the equations of motion for the coherent state amplitudes it is justified to set $X = X_j = N_j = 1$ from the beginning.

Therefore the Euler–Lagrange equations for the b_k^* together with (ν is again the number of electrons in the system, which is constant in time)

$$P_{nm} = \sum_j o_j c_{nj} c_{mj}^* \qquad \sum_n P_{nn} = \nu \tag{A43}$$

yield the equations of motion

$$\mathrm{i}\hbar \dot{b}_k = \hbar\omega_k \left[b_k + \sum_n (B_{nk} P_{n+1,n} + B_{n-1,k} P_{n-1,n}) \right]. \tag{A44}$$

With the help of

$$\mathrm{Re}\,[b_k] = \sum_n \sqrt{\frac{M\omega_k}{2\hbar}} V_{nk} q_n \qquad \mathrm{Im}\,[b_k] = \sum_n \sqrt{\frac{1}{2\hbar M\omega_k}} V_{nk} p_n \tag{A45}$$

(A44) can easily be shown to be equivalent to

$$\dot{p}_n = K(q_{n+1} - 2q_n + q_{n-1}) + 2\alpha\,\mathrm{Re}\,[P_{n,n+1} - P_{n,n-1}]. \tag{A46}$$

From this we see that the dynamics of the lattice (without electron–phonon coupling) follow from the classical equations of motion; however, in contrast to the adiabatic model the dynamics of the electrons are taken explicitly into account. Note that (A46) is identical to the lattice equations in the adiabatic case, since

$$2\alpha\,\mathrm{Re}\,[P_{n,n+1} - P_{n,n-1}] = -\frac{\partial E_\pi}{\partial q_n} \tag{A47}$$

if E_π and $\mathbf{P}$ are determined by diagonalization of the Hückel matrix for geometry $\{q_n\}$, however, in the $|\Phi_2\rangle$ case the MO coefficients are determined in a different way. Temperature effects can be included in the same way as described in appendix F of [71], by introduction of random forces and friction in the above equations in the same way as in the classical case (see appendix F of [71]):

$$\dot{p}_n = K(q_{n+1} - 2q_n + q_{n-1}) + 2\alpha\,\mathrm{Re}\,[P_{n,n+1} - P_{n,n-1}] + R_n(t) - \Gamma p_n. \tag{A48}$$

Thus after renaming d_{nj} to c_{nj} again we arrive at the final equations of motion:

$$\mathrm{i}\hbar \dot{c}_{nj} = (\beta + E_n) c_{n+1,j} + (\beta + E_{n-1}) c_{n-1,j} \tag{A49}$$

where E_n is given by

$$E_n = \sum_k \hbar\omega_k B_{nk}(b_k + b_k^*) = -\alpha(q_n - q_{n+1}) \tag{A50}$$

and thus we obtain

$$\mathrm{i}\hbar \dot{c}_{nj} = [\beta - \alpha(q_n - q_{n+1})] c_{n+1,j} + [\beta - \alpha(q_{n-1} - q_n)] c_{n-1,j}. \tag{A51}$$

The conservation of total energy can be easily shown since we have a Hamiltonian system with time independent Hamilton operator.

With the equations of motion for the coherent state amplitudes we can also simplify our integrand in the phase considerably:

$$\frac{\mathrm{i}\bar{h}}{2}\sum_k(\dot{b}_k b_k^* - \dot{b}_k^* b_k) = \sum_k \bar{h}\omega_k |b_k|^2 + \frac{1}{2}\sum_n (E_n P_{n+1,n} + E_{n-1}P_{n-1,n}) \tag{A52}$$

and therefore

$$\begin{aligned}\sum_j o_j C_j &= -\frac{\mathrm{i}\bar{h}}{2}\sum_k(\dot{b}_k b_k^* - \dot{b}_k^* b_k) + \sum_k \bar{h}\omega_k |b_k|^2 = -\frac{1}{2}\sum_n (E_n P_{n+1,n} + E_{n-1}P_{n-1,n}) \\ &= -\sum_n E_n \,\mathrm{Re}\,[P_{n+1,n}]. \end{aligned}\tag{A53}$$

Thus we can write down our final state vector

$$\begin{aligned} |\psi\rangle &= \frac{1}{\sqrt{\nu!}}\,\mathrm{e}^{-\mathrm{i}/\bar{h}Dt}\,\mathrm{e}^{\mathrm{i}/\bar{h}\int_0^t \vartheta(t')\,\mathrm{d}t'}\sum_P (-1)^p \hat{P}\prod_{j=1}^{\nu}\left[\sum_n c_{nj}\hat{c}_{nj}^+|0\rangle_e\right]|\beta(t)\rangle \\ \vartheta(t) &= \frac{1}{2}\sum_n (E_n P_{n+1,n} + E_{n-1}P_{n-1,n}) \\ D &= \frac{1}{2}\sum_k \bar{h}\omega_k - (N-1)\frac{A^2}{2K} \\ |\beta(t)\rangle &= \mathrm{e}^{\sum_k [b_k(t)\hat{b}_k^+ - b_k^*(t)\hat{b}_k]}|0\rangle_p \end{aligned}\tag{A54}$$

where here j runs over the occupied spin orbitals again.

Note that the expectation values of displacements and momenta derived from this state are exactly the same as those calculated from the classical exact solution discussed above. The same holds also for all expectation values of electronic operators with the state vector at the same time both in the bra and the ket. However, expectation values with the state at different times in the bra and the ket, respectively, as necessary in spectroscopy, would yield different results when calculated with the two states. For example, the autocorrelation function as explained above for the classical solution is given by

$$S(t) = \langle\psi(0)\mid\psi(t)\rangle = \mathrm{e}^{-\mathrm{i}/\bar{h}Dt}\,\mathrm{e}^{\mathrm{i}/\bar{h}\int_0^t \vartheta(t')\,\mathrm{d}t'}\langle\beta(0)\mid\beta(t)\rangle\langle\Delta(0)\mid\Delta(t)\rangle \tag{A55}$$

with

$$\langle\beta(0)\mid\beta(t)\rangle = \exp\left\{-\frac{1}{2}\sum_k[|b_k(0)|^2 + |b_k(t)|^2 - 2b_k^*(0)b_k(t)]\right\}. \tag{A56}$$

The situation this is somewhat similar to the case of Davydov's solitons.

Appendix B.

Note that in our previous paper [71] some misprints occurred (author's mistakes): equation (B24) should read

$$D(\boldsymbol{b}_1, \boldsymbol{b}_2) = \exp\left[-\frac{1}{2}\sum_k(|\boldsymbol{b}_1 - \boldsymbol{b}_2|^2 - \boldsymbol{b}_1^+\boldsymbol{b}_2 + \boldsymbol{b}_2^+\boldsymbol{b}_1)\right]. \tag{B24}$$

(B25) should read

$$D(\boldsymbol{b}_1, \boldsymbol{b}_2) = \exp\left\{-\frac{1}{2}\sum_k[|b_{nk1} - b_{n+1,k1}|^2 - (b_{nk1}^* + b_{mk2}^* + b_{lk3}^*)(b_{n+1,k1} + b_{mk2} + b_{lk3})\right.$$

$$+(b_{nk1}+b_{mk2}+b_{lk3})(b^*_{n+1,k1}+b^*_{mk2}+b^*_{lk3})]\Big\}. \tag{B25}$$

(B26) should read

$$D_{n,n+1,j}=\exp\left[-\frac{1}{2}\sum_k(|b_{nkj}-b_{n+1,kj}|^2-b^*_{nkj}b_{n+1,kj}+b_{nkj}b^*_{n+1,kj})\right]. \tag{B26}$$

(B27*a*) should read

$$\begin{aligned}D(\boldsymbol{b}_1,\boldsymbol{b}_2)=D_{n,n+1,1}\exp\Big\{&+\frac{1}{2}\sum_k[b^*_{nk1}(b_{mk2}+b_{lk3})+(b^*_{mk2}+b^*_{lk3})(b_{n+1,k1}+b_{mk2}+b_{lk3})\\&-b_{nk1}(b^*_{mk2}+b^*_{lk3})-(b_{mk2}+b_{lk3})(b^*_{n+1,k1}+b^*_{mk2}+b^*_{lk3})]\Big\}\\=D_{n,n+1,1}\exp\Big\{&+\frac{1}{2}\sum_k[(b^*_{nk1}b_{mk2}+b^*_{mk2}b_{n+1,k1})-(b_{nk1}b^*_{mk2}+b_{mk2}b^*_{n+1,k1})]\Big\}\\\times\exp\Big\{&-\frac{1}{2}\sum_k[(b^*_{nk1}b_{lk3}+b^*_{lk3}b_{n+1,k1})-(b_{nk1}b^*_{lk3}+b_{lk3}b^*_{n+1,k1})]\Big\}.\end{aligned} \tag{B27}$$

The first two lines of (B29) should read

$$\begin{aligned}D_{n,n+1,j}&=\exp\Big\{-\frac{1}{2}\sum_k[|b_{nkj}-b_{n+1,k,j}|^2-b^*_{nkj}b_{n+1,kj}+b_{nkj}b^*_{n+1,kj}]\Big\}\\D^{mj'}_{nj}&=\exp\Big\{+\frac{1}{2}\sum_k[b^*_{nkj}b_{mkj'}-b_{nkj}b^*_{mkj'}]\Big\}.\end{aligned} \tag{B29}$$

Further (C46) should read

$$\begin{aligned}\frac{\partial D_{m,m+1,j'}}{\partial b^*_{nkj}}&=\left[b_{n+1,kj}\delta_{mn}-\frac{1}{2}b_{nkj}(\delta_{mn}+\delta_{m,n-1})\right]D_{m,m+1,j}\delta_{jj'}\\\frac{\partial D_{m+1,mj'}}{\partial b^*_{nkj}}&=\left[b_{n-1,kj}\delta_{n,m+1}-\frac{1}{2}b_{nkj}(\delta_{mn}+\delta_{m,n-1})\right]D_{m+1,m,j}\delta_{jj'}.\end{aligned} \tag{C46}$$

(C49) should read

$$\begin{aligned}\frac{\partial}{\partial b^*_{nkj}}D^{m'j''}_{mj'}&=\left[+\frac{1}{2}b_{m'kj''}\delta_{nm}\delta_{jj'}-\frac{1}{2}b_{mkj'}\delta_{nm'}\delta_{jj''}\right]D^{m'j''}_{mj'}\\\frac{\partial}{\partial b^*_{nkj}}(D^{m'j''}_{m+1,j'})^*&=\left[-\frac{1}{2}b_{m'kj''}\delta_{n,m+1}\delta_{jj'}+\frac{1}{2}b_{m+1,kj'}\delta_{nm'}\delta_{jj''}\right](D^{m'j''}_{m+1,j'})^*.\end{aligned} \tag{C49}$$

Then in the subsequent equations one has to realize that any occurring $D^{m'j''}_{mj'}$ has to be replaced by $(D^{m'j''}_{mj'})^*$.

References

[1] Su W P, Schrieffer J R and Heeger A J 1979 *Phys. Rev. Lett.* **42** 1698
Su W P 1980 *Solid State Commun.* **35** 899
Su W P, Schrieffer J R and Heeger A J 1980 *Phys. Rev.* B **22** 2099
Heeger A J, Kivelson S, Schrieffer J R and Su W P 1988 *Rev. Mod. Phys.* **60** 781

[2] Thomann H, Dalton L R, Tomkiewicz Y, Shiren N S and Clarke T C 1983 *Phys. Rev. Lett.* **50** 533

Thomson H, Kim H, Morrobel-Sosa A, Dalton L R, Jones M T, Robinson B H, Clarke T C and Tomkiewicz Y 1984 *Synth. Met.* **9** 255
Thomann H, Cline J E, Hofmann B M, Kim H, Morrobel-Sosa A, Robinson B H and Dalton L R 1985 *J. Phys. Chem.* **89** 1994
Heeger A J and Schrieffer J R 1983 *Solid State Commun.* **48** 207
Soos Z G and Ramashesha S 1983 *Phys. Rev. Lett.* **51** 2374
[3] Sasai M and Fukutome H 1984 *Synth. Met.* **9** 295
[4] Orenstein J and Baker G L 1982 *Phys. Rev. Lett.* **49** 1043
Weinberger B R 1983 *Phys. Rev. Lett.* **50** 1693
Blanchet G B, Fincher C P and Heeger A J 1983 *Phys. Rev. Lett.* **51** 2132
Blanchet G B, Fincher C P, Chung T C and Heeger A J 1983 *Phys. Rev. Lett.* **50** 1938
[5] Bishop A R, Campbell D K, Lomdahl P S, Horovitz B and Phillpot S R 1984 *Phys. Rev. Lett.* **52** 671
[6] Wang C L and Martino F 1986 *Phys. Rev.* B **34** 5540
[7] Su W P 1986 *Phys. Rev.* B **34** 2988
[8] Kivelson S and Wu W-K 1986 *Phys. Rev.* B **34** 5423
[9] Su W P and Schrieffer J R 1980 *Proc. Natl Acad. Sci. USA* **77** 5626
[10] Förner W, Seel M and Ladik J 1986 *Solid State Commun.* **57** 463
[11] Förner W, Seel M and Ladik J 1986 *J. Chem. Phys.* **84** 5910
[12] Liegener C-M, Förner W and Ladik J 1987 *Solid State Commun.* **61** 203
Godzik A, Seel M, Förner W and Ladik J 1986 *Solid State Commun.* **60** 609
Orendi H, Förner W and Ladik J 1988 *J. Chem. Phys.* **150** 113
[13] Förner W 1987 *Solid State Commun.* **63** 941
[14] Gibson H W, Weagley R J, Mosher R A, Kaplan S, Prest W M and Epstein A J 1985 *Phys. Rev.* B **31** 2338
[15] Förner W, Wang C-L, Martino F and Ladik J 1988 *Phys. Rev.* B **37** 4567
[16] Boudreaux D S, Chance R R, Bredas J L and Silbey R 1983 *Phys. Rev.* B **28** 6927
[17] Phillpot S R, Baeriswyl D, Bishop A R and Lomdahl P S 1987 *Phys. Rev.* B **35** 7533
[18] Markus R, Förner W and Ladik J 1988 *Solid State Commun.* **68** 1
[19] Förner W 1991 *Phys. Rev.* B **44** 11 743
[20] Förner W 1992 *Chem. Phys.* **160** 173
Förner W 1992 *Chem. Phys.* **160** 188
[21] Nakahara M and Maki K 1982 *Phys. Rev.* B **25** 7789
[22] Rukh R, Sigmund R and Eisele H 1989 *J. Chem. Phys.* **90** 6463
[23] Davydov A S and Kislukha N I 1973 *Phys. Status Solidi* b **59** 465
Davydov A S 1979 *Phys. Scr.* **20** 387
[24] Davydov A S 1980 *Zh. Eksp. Teor. Fiz.* **78** 789 (Eng. transl. *Sov. Phys.–JETP* **51** 397)
[25] 1992 *Habilitation Thesis* University Erlangen–Nürnberg
Förner W 1994 *J. Phys.: Condens. Matter* **6** 9089
[26] Förner W 1993 *J. Phys.: Condens. Matter* **5** 803
[27] Skrinjar M J, Kapor D V and Stojanovic S D 1988 *Phys. Rev.* A **38** 6402
[28] Mechtly B and Shaw P B 1988 *Phys. Rev.* B **38** 3075
[29] Förner W 1992 *J. Phys.: Condens. Matter* **4** 1915
[30] Förner W 1993 *J. Phys.: Condens. Matter* **5** 3883
[31] Motschmann H, Förner W and Ladik J 1989 *J. Phys.: Condens. Matter* **1** 5083
Förner W and Ladik J 1990 *Davydov's Soliton Revisited* ed P L Christiansen and A C Scott (New York: Plenum) p 267
[32] Förner W 1991 *J. Phys.: Condens. Matter* **3** 4333
Förner W 1992 *J. Comput. Chem.* **13** 275
Förner W 1992 *Nanobiology* **1** 413
[33] Davydov A S 1979 *Teor. Mat. Fiz.* **40** 408
Davydov A S 1988 *Phys. Status Solidi* b **146** 619
Davydov A S 1989 *Nonlinearity* **2** 383
[34] Abramowitz A and Stegun I A 1970 *Handbook of Mathematic Functions* 9th edn (New York: Dover) pp 896–897
[35] Förner W 1989 *Synth. Met.* **30** 135
[36] Förner W 1994 *Adv. Quantum Chem.* **25** 207
Förner W 1997 *Ind. J. Chem.* A **36** 355
[37] Schinke R and Engel V 1990 *J. Chem. Phys.* **93** 3252
[38] Majewski J A and Vogl P 1992 *Phys. Rev.* B **46** 12 119

Majewski J A and Vogl P 1992 *Phys. Rev.* B **46** 12 235
[39] Ambrosch-Draxl C, Majewski J A, Vogl P and Leising G 1995 *Phys. Rev.* B **51** 9668
[40] Slater J C 1974 *Quantum Theory of Molecules and Solids* vol 4 (New York: McGraw-Hill)
[41] Becke A D 1988 *Phys. Rev.* A **38** 3098
[42] Becke A D 1993 *J. Chem. Phys.* **98** 5648
[43] Vosko S H, Wilk L and Nusair M 1980 *Can. J. Phys.* **58** 1200
[44] Lee C, Yang W and Parr R G 1988 *Phys. Rev.* B **37** 785
[45] Perdew J P and Wang Y 1986 *Phys. Rev.* B **33** 8800
[46] Bakhshi A K and Ladik J 1994 *Ind. J. Chem.* **13** 494
[47] Bakhshi A K 1992 *Superlatt. Microstruct.* **11** 465
[48] Bakhshi A K 1992 *Annu. Rep. R. Soc. Chem.* C **89** 147
[49] Bakhshi A K and Ladik J 1989 *J. Synth. Met.* **30** 115
[50] Bakhshi A K, Yamaguchi Y, Ago H and Yamabe T *Synth. Met.* at press
[51] Bakhshi A K, Ago H, Yoshizawa K, Tanaka K and Yamabe T 1996 *J. Chem. Phys.* **104** 5528
[52] Ladik J 1988 *Quantum Theory of Polymers as Solids* (New York: Plenum)
[53] Kopidakis B, Soukoulis C M and Economou E N 1995 *Phys. Rev.* B **51** 15 038
[54] König G and Stollhoff G 1990 *Phys. Rev. Lett.* **65** 1239
[55] Suhai S 1994 *Phys. Rev.* B **50** 14 791
Suhai S 1995 *Phys. Rev.* B **51** 16 553
[56] Villar H O, Dupuis M, Watts J D, Hurst G J B and Clementi E 1988 *J. Chem. Phys.* **88** 1003
Villar H O, Dupuis M and Clementi E 1988 *J. Chem. Phys.* **88** 5252
Villar H O, Dupuis M and Clementi E 1988 *Phys. Rev.* B **37** 2520
[57] Amos T and Snyder L C 1964 *J. Chem. Phys.* **41** 1773
[58] Martino F and Ladik J 1970 *J. Chem. Phys.* **52** 2262
Martino F and Ladik J 1971 *Phys. Rev.* A **3** 862
Mayer I, Ladik J and Biczo G 1973 *Int. J. Quantum Chem.* **7** 583
Rosenberg M and Martino F 1975 *J. Chem. Phys.* **63** 5354
[59] Kovar T 1986 *Master's Thesis* University Erlangen–Nürnberg
[60] Förner W 1991 *Phys. Rev.* B **44** 11 743
Förner W 1993 *J. Mol. Struct. (Theochem)* **282** 235
[61] Soos Z G and Ramashesha S 1983 *Phys. Rev. Lett.* **51** 2374
[62] Suhai S 1983 *Habilitation Thesis* Friedrich-Alexander-University Erlangen–Nürnberg
[63] Suhai S 1983 *Phys. Rev.* B **27** 3506
[64] Suhai S 1984 *Phys. Rev.* B **29** 4570
[65] Suhai S 1984 *Int. J. Quant. Chem.* **QBS11** 223
[66] Cruzeiro-Hansson L, Okhonin V A, Khlebopros R G and Yassievich I N 1992 *Nanobiology* **1** 395
[67] Cruzeiro-Hansson L 1994 *Phys. Rev. Lett.* **73** 2927
[68] Heller E J 1978 *J. Chem. Phys.* **48** 2067
[69] Förner W *Phys. Scr.* submitted
[70] Utz W and Förner W *J. Mol. Mod.* at press
[71] Förner W 1994 *J. Phys.: Condens. Matter* **6** 9089